Wan *et al. Energy Mater.* **2025**, *5*, 500090
DOI: 10.20517/energymater.2024.301

Energy Materials

Review

Open Access

Check for updates

Recent progress and challenges of high-loading cathodes for aqueous Zn-ion batteries

Jiajun Wan[1], Hongjiang Song[1], Jiyang Tian[1], Shengkui Zhong[2], Jie Liu[1,*]

[1]Youth Innovation Team of Shandong Higher Education Institutions, College of Chemical Engineering, Qingdao University of Science and Technology, Qingdao 266042, Shandong, China.
[2]Faculty of Civil Engineering, Guangxi Technological College of Machinery and Electricity, Nanning 530007, Guangxi, China.

[*]**Correspondence to:** Dr. Jie Liu, Youth Innovation Team of Shandong Higher Education Institutions, College of Chemical Engineering, Qingdao University of Science and Technology, No.53 Zhengzhou Road, Shibei District, Qingdao 266042, Shandong, China. E-mail: jie.liu@qust.edu.cn

How to cite this article: Wan, J.; Song, H.; Tian, J.; Zhong, S.; Liu, J. Recent progress and challenges of high-loading cathodes for aqueous Zn-ion batteries. *Energy Mater.* **2025**, *5*, 500090. https://dx.doi.org/10.20517/energymater.2024.301

Received: 25 Dec 2024 **First Decision:** 10 Jan 2025 **Revised:** 24 Jan 2025 **Accepted:** 7 Feb 2025 **Published:** 23 Apr 2025

Academic Editor: Bin Wang **Copy Editor:** Ping Zhang **Production Editor:** Ping Zhang

Abstract

Owing to the advantages of low cost, rich resources, and intrinsic safety, aqueous Zn-ion batteries have attracted broad attention as the promising energy storage technology for large-scale smart grids. The cathodes for aqueous Zn-ion batteries have developed rapidly, including Mn-based cathodes, V-based cathodes, and halogen cathodes. High specific capacity and long cycling lifespan have been achieved. However, when the mass loading for cathode materials is scaled up to the practical level, the cycling stability and rate property of aqueous Zn-ion batteries are very unsatisfactory. Therefore, in this review, we deeply analyze the key issues that limit the electrochemical performance of high-loading cathodes for aqueous Zn-ion batteries. Subsequently, we comprehensively summarize the effective solutions to the above issues, including (1) rational binder design, (2) three-dimensional cathode design, (3) cathode material structural optimization, and (4) interface engineering for Zn anodes. Finally, we give a critical perspective from commercial application for the future development of high-loading cathodes for high-energy-density aqueous Zn-ion batteries.

Keywords: Aqueous Zn-ion battery, high areal capacity, developing strategy, commercial application

INTRODUCTION

The increasingly severe energy crisis and environmental problems have forced the rapid development of

renewable clean energy, including solar energy, wind power, *etc.* However, the variability in time and space of renewable clean energy makes their direct application impracticable. High-efficiency energy storage systems are urgently required. Battery-based energy storage has been considered as a promising and large-scale energy storage technology[1-3]. Owing to their high energy density and long cycling life, Li-ion batteries have occupied the main energy storage market, including portable electronic equipment and electric vehicles[4-6]. However, the high cost and uneven distribution of Li resources and the flammable organic electrolyte seriously hinder the application of Li-ion batteries in large-scale energy storage[7-9].

Aqueous Zn-ion batteries (AZIBs), featured by the Zn-based anodes and aqueous electrolytes, possess the advantages of low cost, abundant resources, and intrinsic safety[10-14]. Recently, AZIBs have attracted broad attention and developed rapidly. Figure 1A shows the number of published academic papers involving "aqueous zinc-ion batteries" from 2020 to 2024, which continuously increases. The zinc metal is usually applied as the anode for AZIBs, which possesses high theoretical capacity of 820 mAh g^{-1} and can avoid the use of a current collector and conductive additive[15-17]. However, the uneven Zn deposition and severe side reactions lead to a limited cycling lifespan of zinc metal anodes[18-21]. To enhance the reversibility and stability of zinc metal anodes, functional coatings and electrolyte optimization have been widely studied[22-27].

The cathodes for AZIBs have also been developed rapidly, including Mn-based cathodes, V-based cathodes, organic-based cathodes, Prussian blue analogs, and so on[28-33]. High specific capacity and long cycling life have been achieved for these cathodes. However, excellent electrochemical performances are usually obtained under low-mass-loading active materials (e.g., 1.0 mg cm^{-2}). Figure 1A displays the number of academic papers involving "aqueous zinc-ion batteries + cathode" and "aqueous zinc-ion batteries + high-loading cathode". One can clearly observe that the development of high-loading cathodes for AZIBs is sluggish. However, the increase of the mass loading on cathodes is crucial to achieve practical high-energy-density AZIBs[34-36], which is a huge difference between laboratory study and practical use. Figure 1B and C displays the relationship between total active material mass ratio (R_{weight}) in full cells and cathode mass loading under different N/P ratios ($R_{N/P}$, ratio of areal theoretical capacity of negative electrode and positive electrode) and E/P ratios ($R_{E/P}$, ratio of electrolyte to cathode in μL mg^{-1}), using MnO_2 as an example[37]. It can be seen that as the cathode mass loading increases, the R_{weight} increases correspondingly. Furthermore, under higher cathode mass loading, the R_{weight} can be increased more significantly when the $R_{N/P}$ and $R_{E/P}$ are decreased. However, the high-loading cathodes suffer from poor structural stability and hysteretic reaction kinetics, resulting in unsatisfactory cycling stability and rate property[38-40]. Therefore, to boost the commercial application of AZIBs, a comprehensive review of the key challenges and effective design strategies for high-loading cathodes is urgently required.

Herein, this review systematically analyzes the main issues on the improvement of the electrochemical performance for high-loading cathodes in AZIBs. Subsequently, we comprehensively summarize the solution strategies to the above key issues, including (1) rational binder design, (2) three-dimensional (3D) cathode design, (3) cathode material structural optimization, and (4) interface engineering for Zn anode. Finally, a perspective on the future development of high-loading cathodes for practical AZIBs is proposed. This review will give an in-depth understanding to boost the development of high-loading cathodes in high-energy-density AZIBs.

CHALLENGES FOR HIGH-LOADING CATHODES

Mechanical instability of the thick coating

As a current large-scale electrode preparation technique, the slurry-coating electrode manufacturing process is implemented by a polymer binder to bond the active particles and conductive carbon together on the

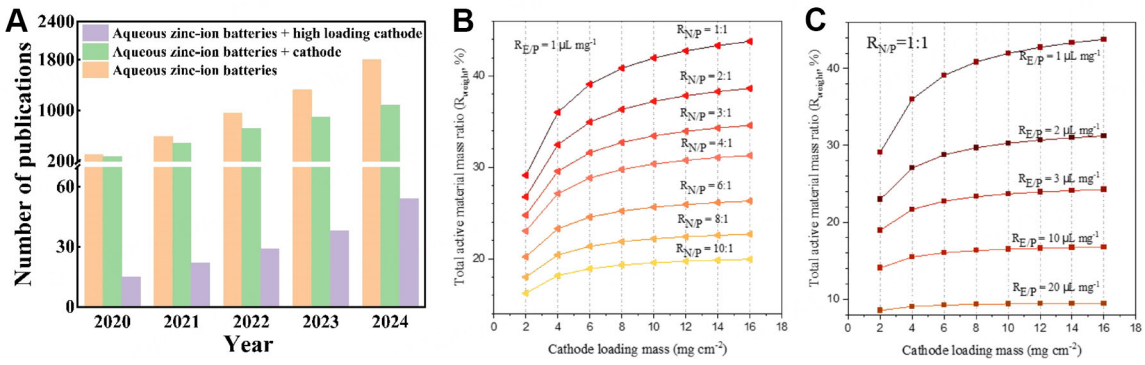

Figure 1. (A) The number of published papers from 2020 to 2024 involving "aqueous zinc-ion batteries", "aqueous zinc-ion batteries + cathode", and "aqueous zinc-ion batteries + high-loading cathode"; Plots of total active material mass ratio R_{weight} in full cell *vs.* cathode mass loading under (B) different $R_{N/P}$ and (C) different $R_{E/P}$, using MnO_2 as an example[37]. Copyright 2024 The Authors.

current collector. Under this process, a large amount of solvent is required as a dispersant. The electrode coating shrinks dramatically with the evaporation of solvent, and thereby huge stress generates interior of the electrode coating during drying. Furthermore, massive Zn^{2+} insertion/extraction causes significant volume change of cathode materials, which aggravates the stress in the electrode coating during cycling. Especially, the commercial linear polyvinylidene difluoride (PVDF) binder can only interact with the active materials and current collector via weak van der Waals forces[41,42], which is incapable of withstanding the huge stress in the high-loading electrodes. As a result, cracks and delamination occur in the high-loading electrodes, leading to a broken conductive network and fast capacity fading.

Sluggish ion transfer in thick electrode

The charge transfer involves two parts, i.e., electron transfer and ion transfer. The electronic conductivity of the electrode has been widely studied, and can be rationally addressed by adding highly conductive additives into the electrodes. However, the sluggish ion transfer in the thick electrodes remains a key issue to achieve high specific capacity for high-loading cathodes under large current density. As the electrode thickness increases, the ion transport distance obviously increases. Meanwhile, the thick electrode coating also leads to insufficient wetting and infiltrating of electrolytes. These result in the inaccessibility of Zn^{2+} into the inner electrode, and thus lower the utilization rate of active materials and specific capacity. At the material level, due to the strong interaction between Zn^{2+} and H_2O, the Zn^{2+} intercalation into the cathode materials involving Zn^{2+} intercalation mechanism (e.g., Mn-based and V-based cathodes) is hindered by the high de-solvation energy barrier of hydrated Zn^{2+}[43,44]. Furthermore, the divalent Zn^{2+} induces strong electrostatic interactions with the cathode hosts, resulting in sluggish solid-state diffusion kinetics as well, compared to the monovalent charge carriers (e.g., Li^+, Na^+)[45,46]. These further exacerbate the unsatisfactory rate property and capacity output of high-loading cathodes.

Dissolution and structural collapse of cathode material

Various cathode materials have been designed for AZIBs, including Mn-based oxides, V-based oxides, Prussian blue analogs, layered chalcogenides, halogens, and organic compounds[47-52]. The Mn-based oxides, V-based oxides, and halogens, possessing high specific capacity and voltage output, have been widely studied. However, in mild-acid aqueous electrolytes (e.g., 2M $ZnSO_4$ aqueous electrolyte), the electrochemical and chemical stability of the metal oxide cathode materials (e.g., MnO_2 and V_2O_5) are challenging with severe dissolution into the electrolyte[53-55]. As a consequence, the cathode materials suffer from fast structural degradation/collapse, leading to the loss of active materials and cell failure. For the cathodes with dissolution mechanism (e.g., I_2 cathodes), although the dissolution of intermediates can boost

the conversion reaction kinetics, the loss of active materials and serious shuttle effect will lead to fast capacity fading and low coulombic efficiency[56-58], which is more severe under high loading.

Incompetent anode stability under high areal capacity

It is a straightforward and effective strategy to achieve high areal capacity by increasing the mass loading on cathodes. As the areal capacity of cathodes increases, the depth of charge/discharge of anodes increases correspondingly. Meanwhile, a low N/P ratio is urgently required for the development of practical AZIBs. The excessive amount of Zn anodes in current studies increases the additional mass of the cells and decreases sharply the energy density. The commercial zinc metal foil is widely used as a Zn anode, as it can avoid additional use of current collector and conductive additive. Due to its intrinsic defects and roughness, the uneven electric field distribution and Zn^{2+} flux lead to heterogeneous Zn deposition and severe dendrites[59,60]. Meanwhile, the competitive hydrogen evolution reaction (HER) and H_2O-induced corrosion on the Zn surfaces cause vast by-products and low coulombic efficiency[61,62]. Unfortunately, under a high depth of charge/discharge, the reversibility and stability of the Zn anodes are further challenged along with massive Zn plating and stripping. Especially, under the limited usage of Zn anodes, the formation of dead Zn is fatal for the capacity output and cycling lifespan of the AZIBs.

It is essential to develop high-loading cathodes for practical AZIBs. However, it is greatly challenging to achieve satisfactory electrochemical performance for high-loading cathodes, as it remains a key issue at both electrode and material levels, which are schematically demonstrated in Figure 2. Therefore, a summary of the effective solutions to the above key issues is timely carried out. The further development direction is discussed thoughtfully.

STRATEGIES FOR DEVELOPING HIGH-LOADING CATHODES

Rational binder design

Polymer binders, as an essential component of traditional electrodes, work to bond the active material and conductive additive together on the current collector. Although the polymer binder accounts for a small amount of the electrode composition, it plays a crucial role in avoiding cracks and maintaining the integration of electrode structure and conductive network. However, the commonly used linear polymer binders (e.g., PVDF) possess inadequate mechanical properties to accommodate the huge stress in high-loading electrodes. As a result, cracks and delamination lead to a short cycling lifespan of high-loading electrodes. Moreover, most of the polymer binders are non-conductive for electrons/ions. This affects the internal resistance of the electrode slightly under low mass loading. However, it will be a non-negligible issue when the mass loading and electrode thickness increase, which significantly reduces the reaction kinetics and rate performance of the battery. Polymer binders have been demonstrated to be crucial for developing high-performance Li-ion batteries and Li-S batteries[63-66]. However, the study of binders for high-performance AZIBs is usually neglected, as shown in Figure 3A. Therefore, the rational binder design strategies for constructing high-loading cathodes in AZIBs are discussed.

Bio-polymer binder

A commercial PVDF binder with symmetrical C-F functional groups possesses poor affinity with the active materials via weak van der Waals forces. Additionally, a toxic and high-cost N-methyl-2-pyrrolidone (NMP) solvent is required for a PVDF binder. Water-based bio-polymers, such as polysaccharides and proteins, contain rich polar functional groups (-COOH, -OH, $-NH_2$, *etc.*)[67-70]. These polar functional groups can firmly anchor the active materials via robust chemical interactions. Besides, their advantages of low cost, abundant resources, and eco-friendliness draw wide attention of researchers. For example, water-based sodium alginate (SA) and xanthan gum (XG) have been explored as the binders for AZIBs[71,72]. The

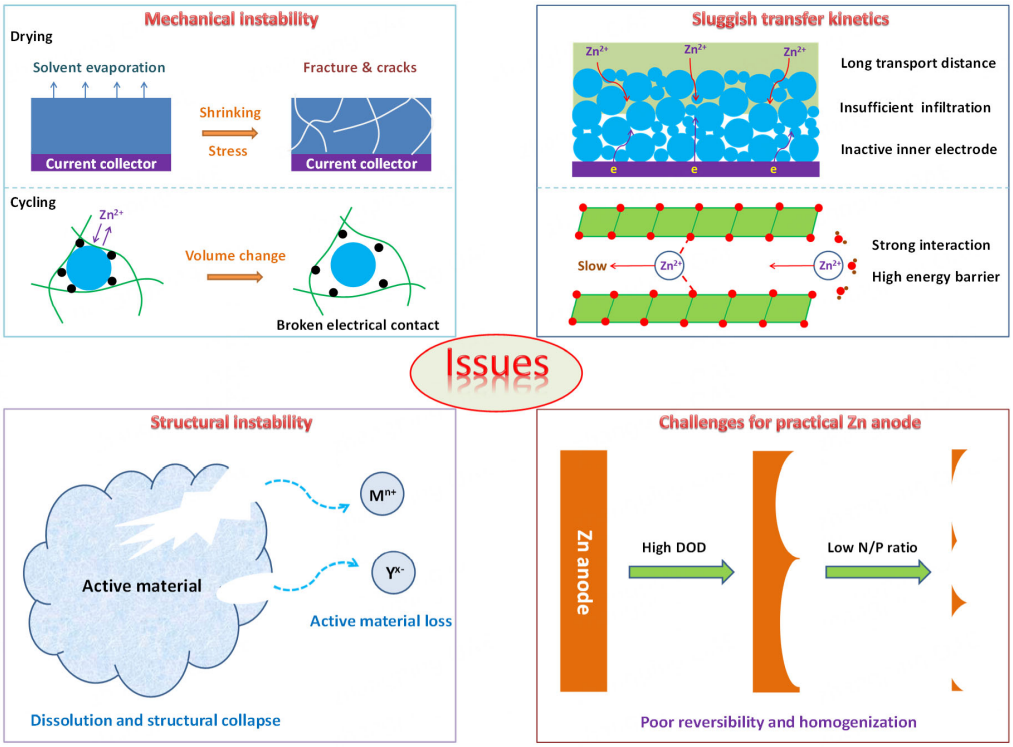

Figure 2. Schematic of the key issues on developing high-performance high-loading AZIBs.

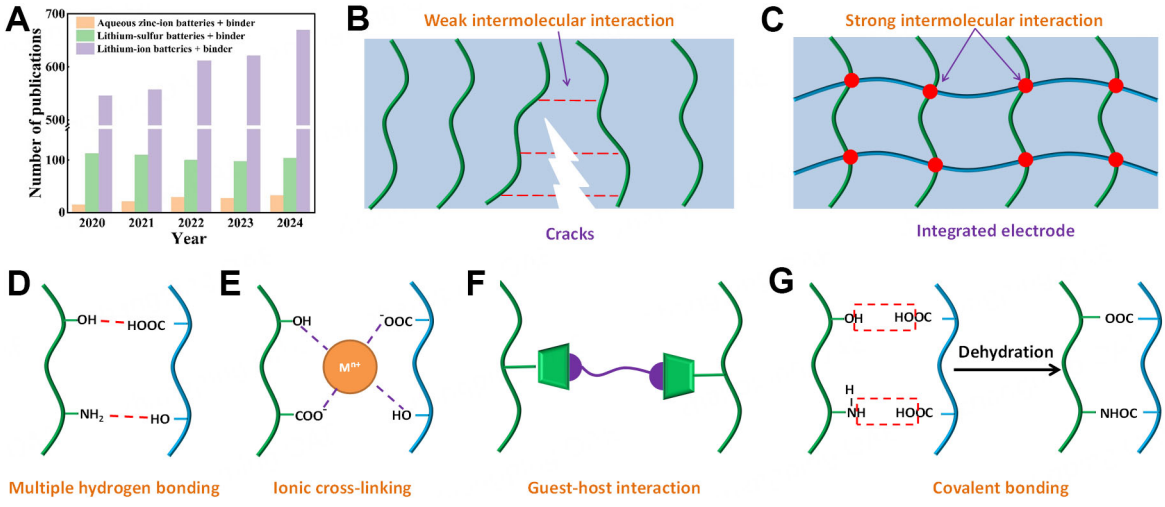

Figure 3. (A) The number of published papers from 2020 to 2024 involving "aqueous zinc-ion batteries + binder", "Lithium-sulfur batteries + binder", and "Lithium-ion batteries + binder"; (B) Schematic of the cracked high-loading electrode using linear binder due to weak intermolecular interactions; (C) Schematic of the integrated high-loading electrode using a mechanically robust network binder; (D-G) Schematic of the strong intermolecular interactions used to construct robust network structures.

water-based bio-polymer binders can make the electrode manufacturing process greener and more sustainable. Nevertheless, the significant swelling of bio-polymer binders in aqueous electrolytes will decrease their mechanical strength. Constructing a network structure is an effective strategy to address the swelling issue. At the same time, the robust network of polymer binders can dramatically enhance its mechanical properties to accommodate the internal stress in high-loading electrodes [Figure 3B and C][73-77].

The common reactions used to construct the robust network binders are displayed in Figure 3D-G, including multiple hydrogen bonding, ionic cross-linking, guest-host interaction, and covalent bonding network.

Conductive binder

The electronic/ionic conductivity of polymer binders plays an important role in the fast charge transfer kinetics in thick high-loading cathodes. Owing to the insufficient wetting and permeation of the electrolyte towards thick electrodes, the ionic transmission in the electrode is very sluggish, leading to low active material utilization rate and specific capacity [Figure 4A], especially under lean electrolyte. The hydrophilic groups (e.g., -COOH, -OH, and -NH_2) in polymer binders can contribute to the increased interfacial wetting between cathode and electrolyte[78-80], and therefore boost interfacial Zn^{2+} transfer kinetics effectively. On the other hand, polymer binders with zincophilic functional groups (e.g., -COO^- and -SO_3^-) can act as an anionic polyelectrolyte to accelerate the Zn^{2+} diffusion [Figure 4B][81,82]. A water-soluble binder combining a polysaccharide SA with a hydrophobic polytetrafluoroethylene (PTFE) has been developed for high-performance MnO_2 cathode[82]. The -COO^- in SA can facilitate the adsorption and transmission of Zn^{2+}, while the hydrophobic PTFE can drive the fast de-solvation of hydrated Zn^{2+}. As a result, the high Zn^{2+} diffusion coefficient as well as fast Zn^{2+} intercalation kinetics enables a high rate performance and specific capacity. Moreover, the SA/PTFE hybrid binder also helps to form a protective layer on MnO_2 cathode, which inhibits the disproportion reaction of Mn^{3+} and improves its stability. To achieve fast electronic conductivity in cathodes, electronic conductive polymers have been exploited as novel binders[83,84]. The conductive polymers generally contain conjugated structures along the polymer backbone to achieve electron mobility. For example, a poly (3,4-ethylene dioxythiophene) : poly (styrene sulfonate) (PEDOT : PSS) system has been widely used as a conductive binder[85]. The introduction of conductive binders in cathodes can also reduce the amount of inactive conductive carbon additive, and thus improve the energy density of the battery.

Multifunctional binder

Multifunctional binders can act as multiple roles in electrodes, and address multiple issues simultaneously. For instance, in I_2 cathodes, the severe shuttle and sluggish conversion kinetics of polyiodide intermediates result in low active material utilization rate and coulombic efficiency[86-88]. Therefore, the functional binder is expected to possess commendable chemisorption and catalytic capability. Wang *et al.*[89] reported a bifunctional polyacrylonitrile copolymer binder (LA133) with strong iodine-chemisorption capability for shuttle-free aqueous Zn-I_2 batteries. Via theoretical calculation, the amide and carboxyl groups in LA133 binder can strongly bond to polyiodides to immobilize them in the cathode matrix [Figure 5A]. As a result, under a high mass loading of 7.82 mg cm^{-2}, the Zn-I_2 battery can still retain 83.3% of its initial capacity after 1000 cycles, which is much superior to the common PTFE binder [Figure 5B]. Owing to the poor iodine-chemisorption capability of PTFE binders, soluble I_3^- species diffuse toward the Zn anode side and react with zinc metal, causing severe Zn anode corrosion and roughening. As a result, serious side reactions on both cathode and anode occur, demonstrated by the scanning electron microscopy (SEM) images of cycled cathodes and Zn anodes [Figure 5C-F]. Yang *et al.*[90] also proposed a Janus functional binder based on chitosan (CTS) molecules to hinder the serious shuttle effect of polyiodides. On the one hand, CTS molecules exhibit a robust double helix structure with strong mechanical properties to withstand the electrode swelling effect. On the other hand, the polar groups (-NH_2, -OH, and -O-) in CTS molecules show a strong affinity with iodine species to hinder their dissolution. Furthermore, these interactions enhance iodine catalytic conversion, effectively mitigating the undesired shuttle effect.

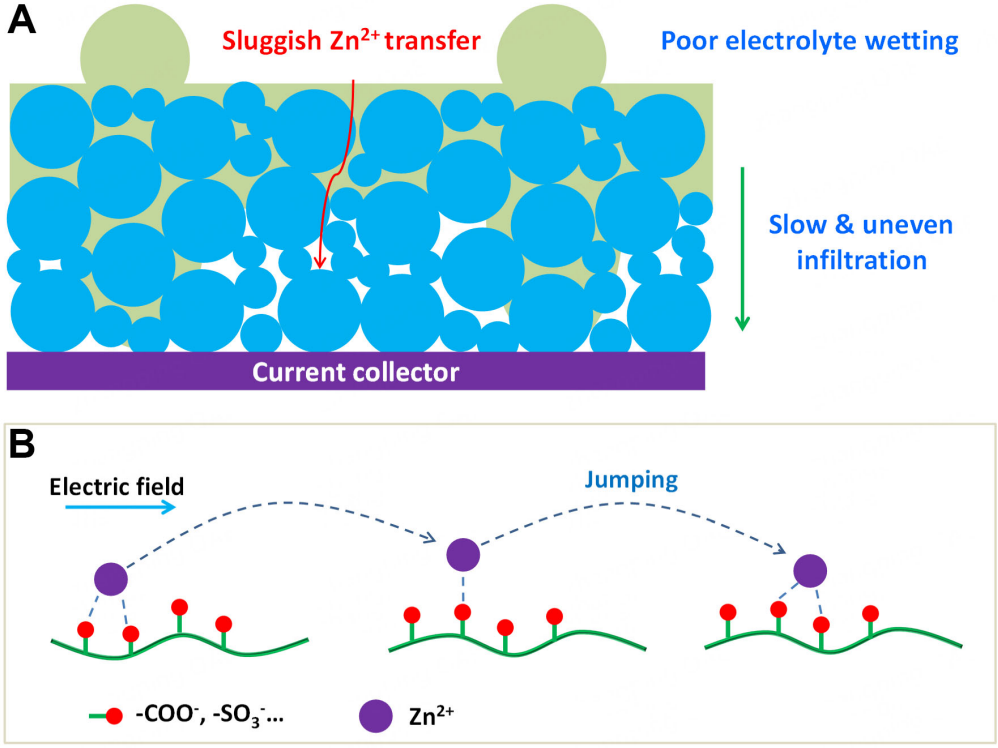

Figure 4. (A) The schematic to show key issues of Zn^{2+} transfer in thick cathodes; (B) The schematic of Zn^{2+} transfer in Zn^{2+}-conducting polymer binders.

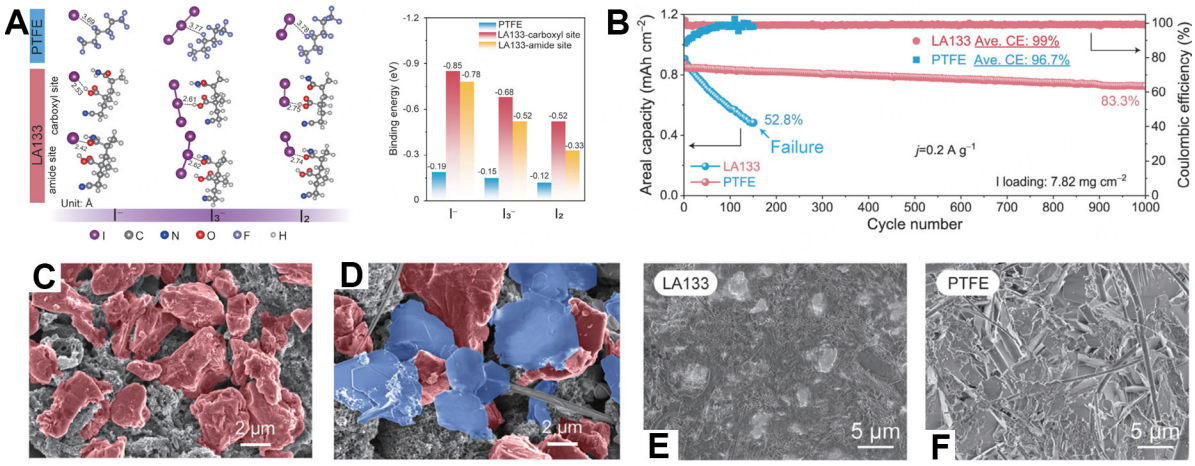

Figure 5. (A) The optimized adsorption configurations and corresponding binding energies of the PTFE binder and LA133 binder to I^-, I_3^-, and I_2 species; (B) Cycling performance of high-loading I_2 cathodes using LA133 binder and PTFE binder; (C and D) SEM images of the cycled cathodes using LA133 binder and PTFE binder, respectively; (E and F) SEM images of the cycled Zn anodes in Zn-I_2 batteries using LA133 binder and PTFE binder, respectively[89]. Copyright 2024 The Authors. PTFE: Polytetrafluoroethylene; SEM: scanning electron microscopy.

This section summarizes the recent advances in the binder design for AZIBs. For constructing high-loading cathodes, the binders should first possess strong mechanical strength to withstand the electrode swelling and huge stress during electrode preparation and battery cycling. Multifunctional binders are a highly significant research direction to address multiple issues in the cathodes, which can further reduce the

amount of inactive functional materials. Above all, water-based bio-polymer binders can make the electrode manufacturing process green and sustainable, and thus should be paid broad attention.

Three-dimensional cathode design

Compared with traditional planar electrodes, 3D electrodes can effectively increase the electrode surface area and active sites, decrease the electrode coating thickness, and shorten the electron/ion transfer distance. Therefore, constructing 3D structured electrodes is another promising and widely reported strategy to achieve high-loading cathodes. This section reviews the main manufacturing techniques for 3D structured cathodes in AZIBs.

Slurry coating

Current collectors act as the electronic and mechanical support to the electrode coating, and play an important role in maintaining the physical structure of the electrode. Coating the cathode slurry into the 3D current collector is a straightforward way to achieve 3D structured electrodes. Carbon-based materials with the advantages of light weight and high electronic conductivity attract wide attention as 3D current collectors[91,92]. For instance, Ma *et al.*[91] constructed high-mass-loading VO_2 electrodes via combining commercial carbon fabric 3D current collectors and PEDOT : PSS conductive binders. Such a strategy provides fast electron transfer and offers sufficient void space to hold active materials and electrolytes. Therefore, the VO_2 loading could reach as high as 15 mg cm^{-2} and the cathode can maintain a capacity of 275 mAh g^{-1}. Biomass, as the sustainable and low-cost raw materials, has been widely used to prepare carbonaceous materials[93-96]. As shown in Figure 6A, Zhao *et al.*[96] directly converted rattan into a carbon-based 3D current collector with directional channels and high compressive strength via an ultraviolet light irradiation-assisted delignification followed by a high-temperature carbonization. Then, a cathode slurry containing carbon nanotube (CNT)/α-MnO_2, conductive carbon, and PVDF binder (7:2:1) was uniformly coated into the as-prepared 3D current collector to achieve a high-mass-loading carbonized rattan CR/MnO_2 cathode, as shown in Figure 6B-F. Owing to the 3D architecture of the CR/MnO_2 cathode that can expose sufficient active sites for Zn^{2+} ion storage, high areal capacity can be achieved under high mass loading, as displayed in Figure 6G and H.

In-situ growth

In-situ growth of 3D-structured active materials on the conductive substrate is another effective strategy to construct 3D electrodes, which avoids the use of additional binder and conductive additive[97-100]. As shown in Figure 7A-C, Chen *et al.*[97] synthesized $V_3O_7{\cdot}H_2O$ nanoarrays (VOHAs) via facile one-step recrystallization of dissolved V_2O_5 from HCl solution on carbon-fiber paper, which was directly used as a binder-free cathode for AZIBs. The open pore structure of the VOHA cathode can boost the electrolyte infiltration and Zn^{2+} transfer. The dependence of the capacities on mass loading was studied as well. Figure 7D displays that the free-standing VOHA cathode can maintain maximal active material utilization with mass loading up to 5.0 mg cm^{-2}. When the mass loading is over 5.0 mg cm^{-2}, specific capacity drops with the increasing mass loading, owing to the decrease in the utilization rate of active materials. Therefore, the rational design for the electrode microstructure is vital. It should be further developed to effectively facilitate ionic/electronic transport and thus decrease such a capacity drop under increasing mass loading. Gao *et al.*[98] reported a $Na_{0.55}Mn_2O_4{\cdot}1.5H_2O$ (NMO) with 3D varying thinness CNT networks (NMO/VTCNTs) as free-standing binder-free cathodes to simultaneously increase the mass loading of the active material and enhance the ionic/electronic conductivity of the electrode. NMO was firstly grown on low-thinness CNTs (LTCNTs, with a diameter of 5-10 nm) via a facile co-precipitation method to obtain NMO/LTCNTs composite. Then, the NMO/VTCNTs free-standing cathode was obtained via suction filtration of NMO/LTCNTs and high-thinness CNTs (HTCNTs, with a diameter of 110-150 nm) solution. The as-prepared NMO/VTCNTs cathodes are able to achieve a loading of about 5 mg cm^{-2} and can

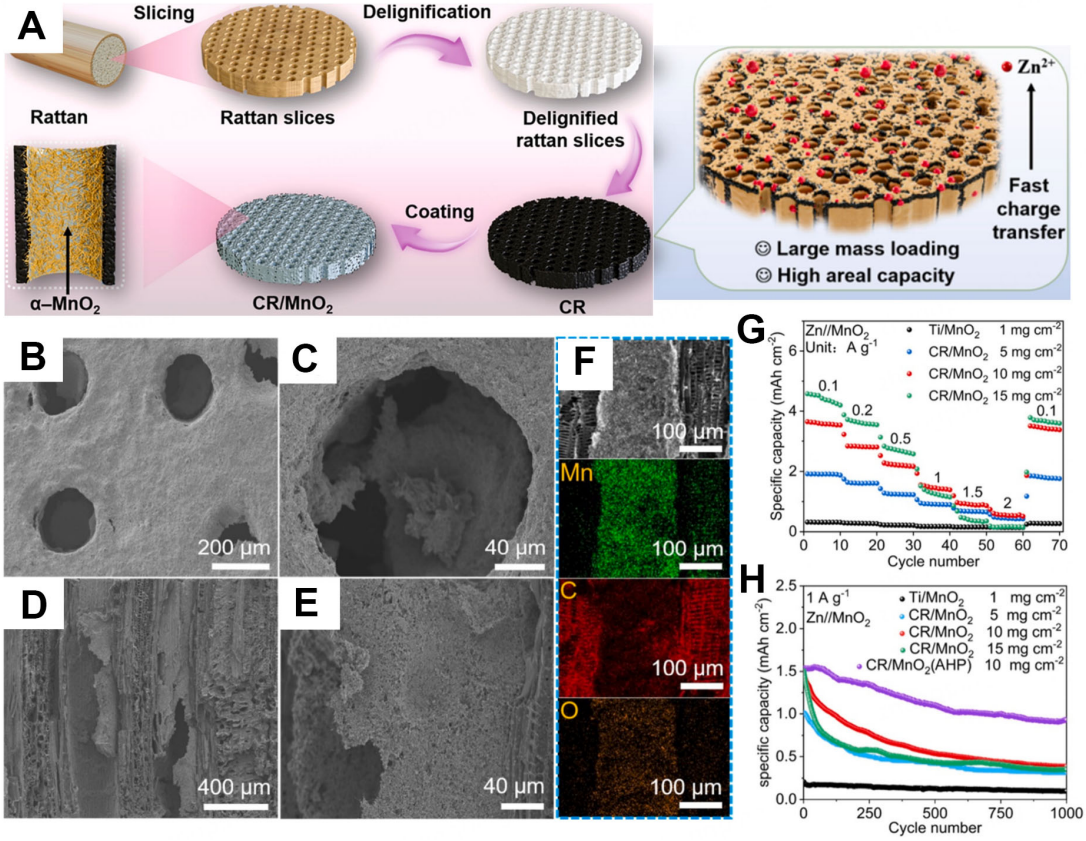

Figure 6. (A) Schematic illustration of the fabrication process of high-loading CR/MnO_2 cathode; (B and C) Top-view and (D and E) cross-section SEM images of CR/MnO_2 cathode; and (F) corresponding EDS mapping images; (G) Rate performance and (H) cycling performance of AZIBs with different MnO_2 cathodes[96]. Copyright 2024 Elsevier Inc. SEM: Scanning electron microscopy; AZIBs: aqueous Zn-ion batteries; EDS: energy dispersive X-ray spectroscopy.

maintain excellent electrochemical performance with a capacity of 158 mAh g^{-1} after 1000 cycles at 2 A g^{-1}.

Novel manufacturing technology

The utilization of a novel electrode preparation process such as 3D printing has also attracted wide attention to construct high-loading electrodes[101-104]. 3D printing technology shows unique manufacturing advantages, such as customized design, rapid prototyping, and structural optimization. Therefore, 3D printing technology has been widely used to fabricate various materials and devices in the fields of energy storage, electronic industry, *etc.* Yang *et al.*[103] prepared a carbon-based 3D current collector [3D-printed carbon microlattices (3DP CMs)] by direct ink 3D printing and subsequent high-temperature annealing. Then, high-loading MnO_2 cathodes can be achieved via electrochemical deposition of MnO_2 on the 3DP CMs. Finally, 28.4 mg cm^{-2} MnO_2 can be loaded on the 3D-printed current collector to deliver an areal capacity of 8.04 mAh cm^{-2} at 0.1 mA cm^{-2}. As shown in Figure 8A and B, Ma *et al.*[104] also manufactured a cellular and hierarchical porous $Fe_5V_{15}O_{39}(OH)_9 \cdot 9H_2O$/reduced holey graphene oxide (FeVO/rHGO) cathode using the direct ink writing technology, where the ink consists of a composite of FeVO and rHGO with PVDF binder. The unique structure with periodic open macro-porous channels and hierarchical porous structures can boost the infiltration of electrolytes. As a result, the mass loading of FeVO/rHGO cathode with four printing layers can reach 24.4 mg cm^{-2}, which can give a remarkably high areal capacity of 7.04 mAh cm^{-2} at 6 mA cm^{-2} [Figure 8C].

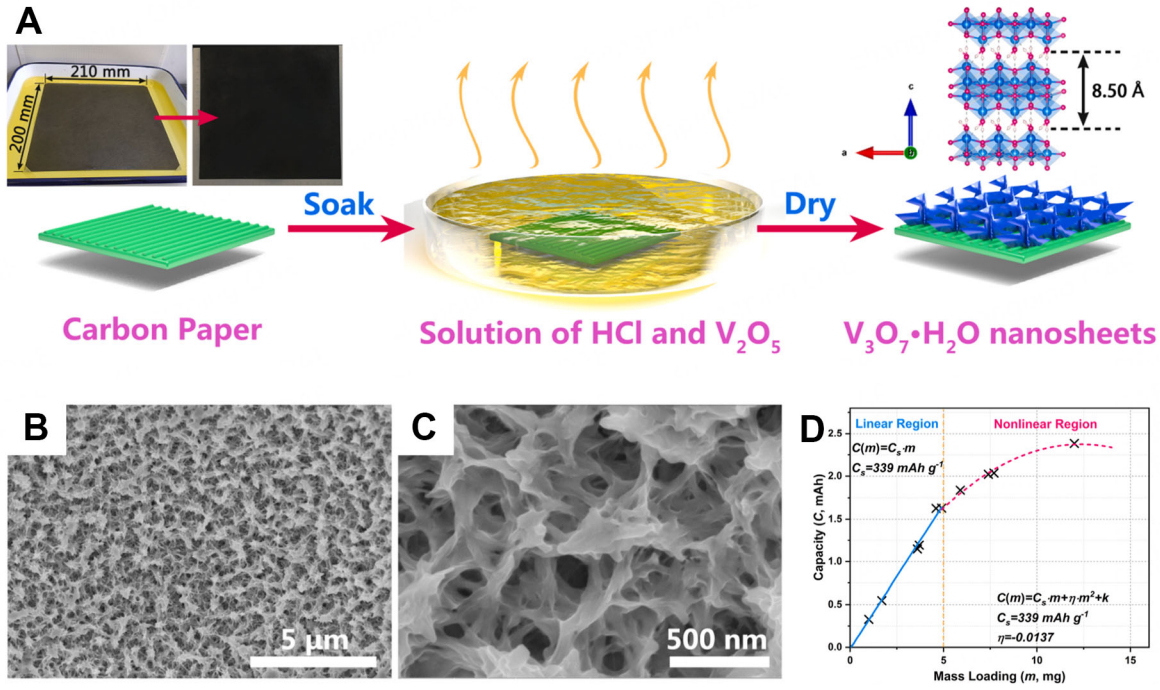

Figure 7. (A) Schematic of the one-step synthesis process for the binder-free VOHAs cathode; and (B and C) the corresponding SEM images; (D) The relationship between the capacity and mass loading of cathode materials[97]. Copyright 2021 Elsevier Ltd. SEM: Scanning electron microscopy; VOHAs: V_3O_7·H_2O nanoarrays.

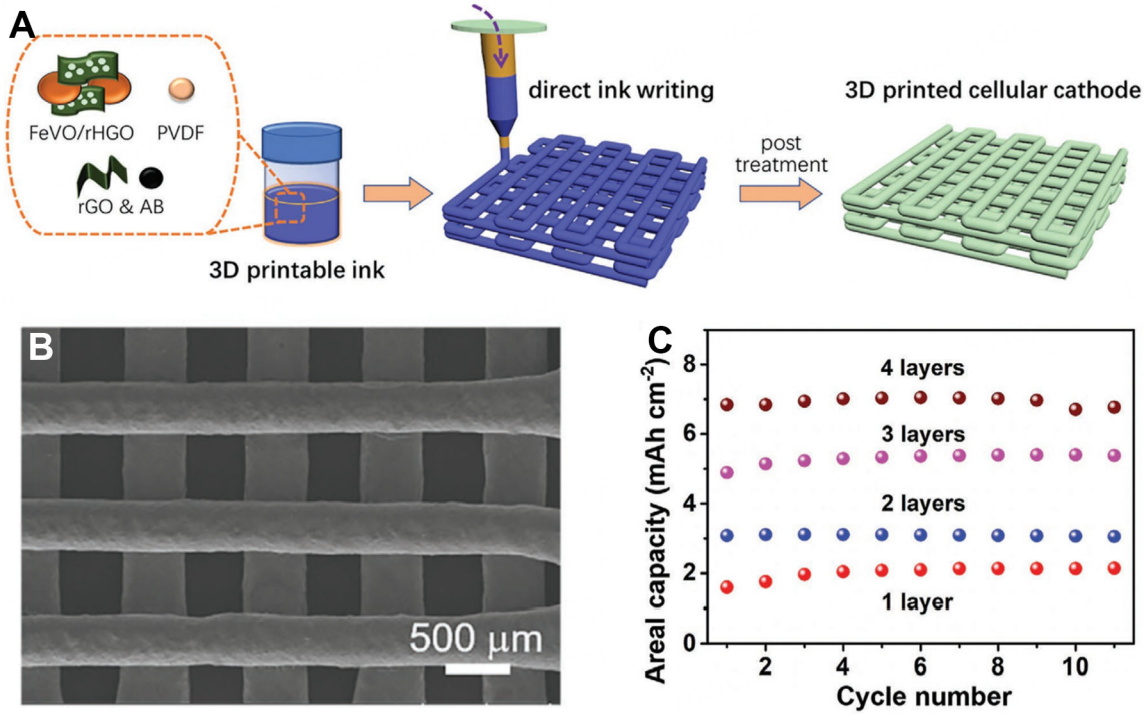

Figure 8. (A) Schematic of direct ink writing fabrication process for the cellular FeVO/rHGO cathode; and (B) corresponding SEM image; (C) The plots of areal capacity of the FeVO/rHGO cathode with different printing layers at 6 mA cm^{-2} [104]. Copyright 2021 Wiley-VCH GmbH.

In summary, this section reviews the progress of high-loading cathodes based on 3D-structured electrodes. The 3D structured electrodes are commonly used to prepare high-loading cathodes in the laboratory study. However, compared to the commercial slurry-casting preparation process on planar current collector, these electrodes usually require additional preparation processes, which will increase the electrode manufacturing cost. Furthermore, the vast inner void space in the 3D structured electrodes will not only increase the electrolyte dosage but also decrease the volumetric energy density. Therefore, the future development of 3D structured electrodes should pay attention to sustainable and large-scale processing techniques. Moreover, the electrode microstructure should be optimized to facilitate ionic/electronic transport and minimize the excess inner void space simultaneously.

Cathode material structural optimization

Surface engineering

Surface engineering with conducting materials has been demonstrated as an effective approach to improve the electronic conductivity and structural stability of active materials[105-108]. Zhang *et al.*[106] reported a graphene-wrapped $H_{11}Al_2V_6O_{23.2}$ nanobelt (HAVO@G) composite, which was prepared by a hydrothermal method and freeze-drying technique. The uniform graphene coating on the surface of HAVO nanobelts can improve electrical conductivity and inhibit the dissolution of the active material into electrolyte, thus leading to enhanced reaction kinetics and structural stability. As a result, the HAVO@G electrode exhibits excellent cycling stability under a high mass loading of 15.7 mg cm^{-2}, delivering a high reversible capacity of 131.7 mAh g^{-1} after 400 cycles at 2 A g^{-1}. Recently, MXenes have attracted extensive attention in AZIBs, owing to their high metallic conductivity and excellent hydrophilicity[109,110]. Furthermore, compared to carbonaceous materials, MXenes possess high density to achieve high-tap-density cathode composite, and thus can improve the volumetric energy density of AZIBs. Shi *et al.*[110] prepared high-density Ti-MXene ($Ti_3C_2T_x$)@MnO_2 micro-flowers via a gas-phase spray drying approach, where MnO_2 nanoparticles are encapsulated in the MXene nanosheets. The $Ti_3C_2T_x$@MnO_2 micro-flowers not only show high tap density of 1.52 g cm^{-3} but also possess fast 3D conductive architecture. As a result, under a mass loading of 8.0 mg cm^{-2}, satisfactory rate property and cycling stability can still be achieved.

Lattice regulation

Lattice regulation of the active material is considered as another effective way to enhance their ionic/electronic conductivity and structural stability[111-115]. Doping/insertion of metal ions is one of the common lattice matrix regulation strategies. Yang *et al.*[112] reported a $Mn_{2.5}V_{10}O_{24}\cdot 5.9H_2O$ (MVOH) cathode material, in which inserted Mn^{2+} can regulate the electronic structure and defective state of the MVOH material. The inserted Mn^{2+} can form new coordination bonds with O atoms in the [VO] layer to regulate the electronic structure, resulting in high electronic conductivity and structural stability [Figure 9A]. Simultaneously, resulting from the insertion of low-valence state Mn^{2+}, abundant O vacancies occur in the MVOH, and thus the electrostatic interactions between Zn^{2+} and the cathode host can be weakened, decreasing Zn^{2+} diffusion energy barrier [Figure 9B]. As a result, the rate property and cycling stability of MVOH cathodes can be obviously improved, as shown in Figure 9C. In particular, the high-loading (~12 mg cm^{-2}) MVOH cathode with synchronously promoted electronic and ionic transport can deliver a high areal capacity of 3.42 mAh cm^{-2} after 850 cycles with a remarkable capacity retaining rate of 91.4 %. Zong *et al.*[113] reported the two-dimensional topological Bi_2Se_3 with Bi-vacancies derived from Cu doping (Cu-$Bi_{2-x}Se_3$) through a one-step hydrothermal process. Density functional theory (DFT) calculations indicate that the formation energy of Bi vacancies for Cu-$Bi_{2-x}Se_3$ is dramatically lowered compared to the pure Bi_2Se_3 sample (1.1 eV *vs.* 3.7 eV). Importantly, the formation of Bi vacancies can effectively enhance the electronic conductivity and reduce the Zn^{2+} migration barrier, resulting in more carrier reversible insertion. Consequentially, the specific capacity of high-loading Cu-$Bi_{2-x}Se_3$ cathodes can be maintained as high as 231.5 mAh g^{-1} and 170.2 mAh g^{-1} after 50 cycles under the mass loading of 6.59 mg cm^{-2} and 10.18 mg cm^{-2},

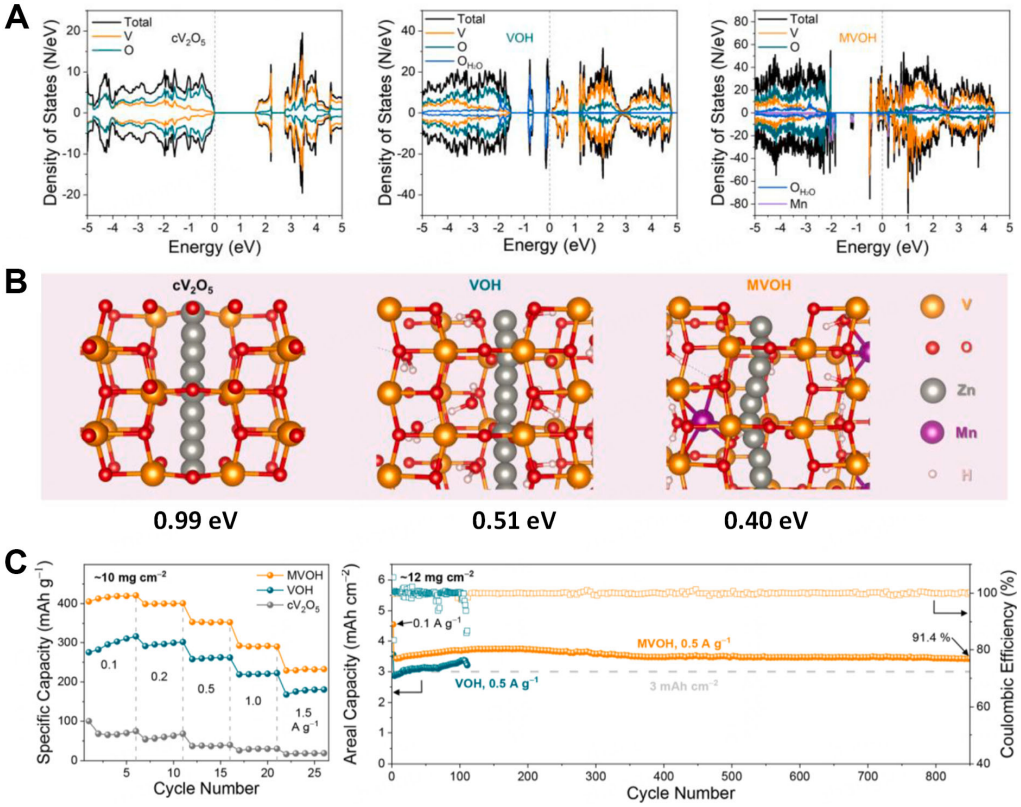

Figure 9. (A) Calculated PDOS and TDOS profiles; and (B) the possible Zn^{2+} migration pathways and calculated diffusion energy barrier in the crystal lattice of cV_2O_5, VOH, and MVOH; (C) Electrochemical performance of the high-loading V-based cathodes[112]. Copyright 2023 Elsevier B.V. MVOH: $Mn_{2.5}V_{10}O_{24}·5.9H_2O$; VOH: $V_{10}O_{24}·6.9H_2O$; PDOS: partial density of states; TDOS: total density of states.

respectively.

Interestingly, the metal ion doping/intercalation can boost the reaction kinetics via an activation effect. For example, a co-intercalation strategy of Na^+ and Cu^{2+} was introduced into δ-MnO_2 (NCMO) by Gao *et al.*[116]. On the one hand, the co-intercalation of Na^+ and Cu^{2+} synergistically modulates the electronic structure of δ-MnO_2 to achieve rapid electronic transfer. On the other hand, the activation effect of Cu^{2+} towards the Mn^{2+}/Mn^{4+} two-electron conversion is amplified by the pre-intercalation of Na^+, resulting in improved specific capacity. Therefore, the NCMO cathode can exhibit a specific capacity as high as 576 mAh g^{-1} under the mass loading of 1.0 mg cm^{-2} and an areal capacity of 2.1 mAh cm^{-2} under the high mass loading of 10.9 mg cm^{-2}.

Molecule/atom engineering

Molecule insertion is another promising approach to expand the interlayer spacing of the cathode host and boost Zn^{2+} transport kinetics[117-119]. Yao *et al.*[118] reported a $MoS_2/C_{19}H_{42}N^+$ (CTAB) superstructure, in which the MoS_2 monolayer is alternately separated by the CTAB layer. Owing to the insertion of CTAB, the interlayer spacing of the layered MoS_2 host increases significantly from 0.63 nm to 1.0 nm [Figure 10A and B]. Specially, due to the close-knit interactions between MoS_2 monolayers and CTAB layers, the stability of the layered structure can be strengthened. Meanwhile, the soft CTAB layer, as a hyperelastic buffer, can effectively alleviate expansion stress and suppress structural collapse, which has been indicated by the *in-situ* synchrotron X-ray diffraction (SXRD) tests in Figure 10C. The high-resolution transmission electron

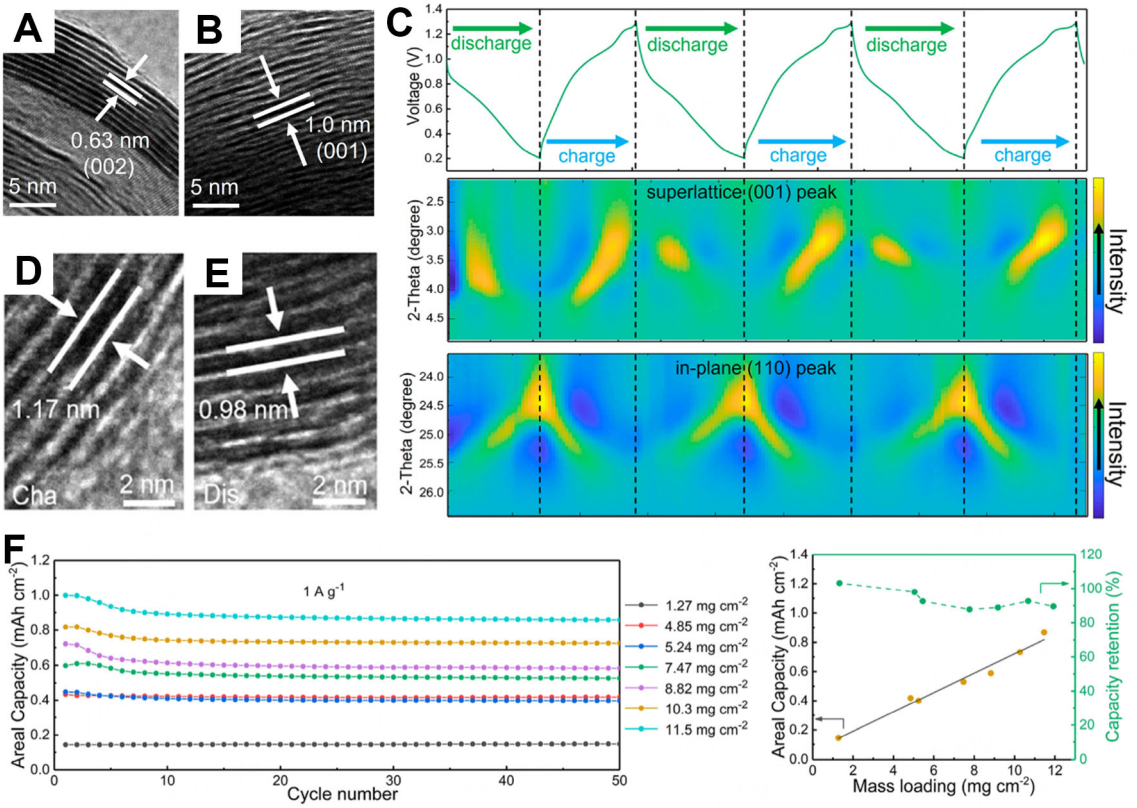

Figure 10. HRTEM images of (A) pristine MoS_2 and (B) MoS_2-CTAB; (C) *In-situ* SXRD tests of the MoS_2-CTAB superstructure during the Zn^{2+} insertion/extraction processes; HRTEM images of MoS_2-CTAB (D) after charging and (E) after discharging; (F) The electrochemical performance of the MoS_2-CTAB superstructure under different mass loading[118]. Copyright 2022 American Chemical Society. HRTEM: High-resolution transmission electron microscopy; SXRD: synchrotron X-ray diffraction; CTAB: $C_{19}H_{42}N^+$.

microscopy (HRTEM) images during cycling further reveal the breathing of the interlayer distance between 0.98 nm and 1.17 nm upon Zn^{2+} insertion/extraction [Figure 10D and E]. Therefore, the MoS_2-CTAB electrode shows enhanced cycling stability with a capacity retention of as high as 92.8% at 10 A g^{-1} over 2100 cycles. Even under a large mass loading of 11.5 mg cm^{-2}, the MoS_2-CTAB electrode can cycle stably over 50 cycles at 1 A g^{-1} [Figure 10F]. Moreover, as the mass loading increases, an almost linear increase in areal capacity can be achieved.

Apart from the high intrinsic ionic conductivity of the cathode host materials, ion transport highway in the electrode level is also of great importance. Jiang *et al.*[120] reported that a sharp capacity shrinkage under high loading can be caused by the formation of vast alkaline zincate [$Zn_4SO_4(OH)_6{\cdot}nH_2O$, ZSH] on the surface of MnO_2 cathode, which blocks the ionic transfer pathway. The H^+/Zn^{2+} co-intercalation in MnO_2 cathodes, which is widely demonstrated, can lead to H^+ consumption and thus shift the acid-base balance in the aqueous electrolyte to continuously produce OH^-. Under high loading, the massive consumption of H^+ can lead to sharp increase of local pH and vast ZSH generation on the cathode/electrolyte interface. The ZSH can fully cover the high-loading MnO_2 cathode, leading to a stagnant electrochemical reaction. To address this issue, they introduced the positively charged interstitial carbon into the lattice matrix of MnO_2 (IC@MnO_2). DFT calculations indicate that IC@MnO_2 possesses lower affinity to SO_4^{2-} and OH^- than that of bare MnO_2, and thereby suppresses the ZSH generation and covering effect. Hence, under a high mass loading of 10 mg cm^{-2}, the IC@MnO_2 cathode can deliver a much higher active material availability and specific capacity than the MnO_2 electrode (176.4 mAh g^{-1} *vs.* 108.5 mAh g^{-1}).

This section summarizes the rational cathode material design strategies for high-loading cathodes. On the one hand, the conductive surface coating can significantly improve electronic conductivity and suppress the collapse of active materials. On the other hand, the lattice matrix regulation of the cathode host effectively adjusts their electronic structure, interlayer spacing, and structural stability. The integrated strategy combining surface coating and lattice regulation should be developed to enhance both apparent and intrinsic conductivity of cathode materials, and thus effectively decrease the capacity shrinkage upon increasing mass loading. For insertion-type cathode materials, the H^+/Zn^{2+} co-intercalation can result in massive ZSH by-products and severe blocking effect. It should be paid wide attention to avoid such covering effect and ensure fast ion transfer on the cathode/electrolyte interface, especially under high mass loading.

Interface engineering for Zn anode

To match the high areal capacity of high-loading cathodes, the high-depth charge/discharge of Zn anodes is required. Furthermore, a low N/P ratio is essential for the practical high energy density of AZIBs. However, under such harsh conditions, the anode/electrolyte interface is quite unstable, owing to the serious dendrite growth, HER, corrosion, and passivation [Figure 11A]. It is urgently required to improve the high reversibility and stability for Zn anodes under high areal capacity. Therefore, this section reviews the effective strategies for developing practical Zn anodes.

Artificial coating

Constructing a solid protective layer is an effective approach to homogenize the Zn^{2+} flux and shield side reactions, as shown in Figure 11A. Various artificial protective films have been constructed by blade-coating, spin-coating, atomic layer deposition and other processes[121-128]. Zhu *et al.*[121] constructed a multifunctional water-glass artificial protective layer containing rich Si-O hydrophilic groups on Zn anode surface via a spin-coating method. The vast polar Si-O functional groups can effectively improve the interfacial wettability, facilitate the even electric field distribution, and guide uniform Zn deposition along the (002) plane. Hong *et al.*[122] coated a cation-exchange membrane of perfluorosulfonic acid on the Zn anode surface, which contains abundant sulfonic acid groups. This cation-exchange membrane can electrostatically repulse the SO_4^{2-} anions while accelerating the uniform Zn^{2+} ion transport. Therefore, the formation of $Zn_4SO_4(OH)_6{\cdot}5H_2O$ by-products can be suppressed and the homogenization of Zn^{2+} distribution on the Zn anode surface can be achieved.

Chen *et al.*[125] constructed a polyvinyl alcohol (PVA)@SO_4^{2-} receptor (SR)-$ZnMoO_4$ multifunctional composite coating on Zn anode with a solid electrolyte interphase (SEI)-like structure. The PVA@SR outer layer with good flexibility can not only improve the coating stability but also effectively bind SO_4^{2-} to hinder its access to the Zn surface. Meanwhile, it finds that the $ZnMoO_4$ inorganic component with high ionic binding energy can effectively enhance the ionic conductivity of the composite coating. Based on these advantages, the Zn anode exhibits high reversibility with a coulombic efficiency of 99.42% and shows a superior high-capacity cycling performance of 1,700 h at 5 mA cm^{-2}/5 mAh cm^{-2}. To shield H_2O molecules, Zhou *et al.*[128] construct a hydrophobic-zincophilic bifunctional layer on Zn anodes, which is synthesized by free radical polymerization of PVDF and acrylic acid. The hydrophobic framework acts as a barrier layer to isolate the Zn anode from the active H_2O molecules in aqueous electrolyte, and thus suppresses the HER and corrosion reactions. Meanwhile, the zincophilic functional groups (-COOH) on the sidechain can form effective transfer pathways for Zn^{2+}, and thus guide uniform Zn deposition. As a result, even under high current density and areal capacity (12 mA cm^{-2} and 6 mAh cm^{-2}), Zn||Zn symmetrical cells can cycle stably for 1,000 h. In sharp contrast, the symmetrical cells with bare Zn anodes are unbearable to harsh conditions and fail after only several cycles.

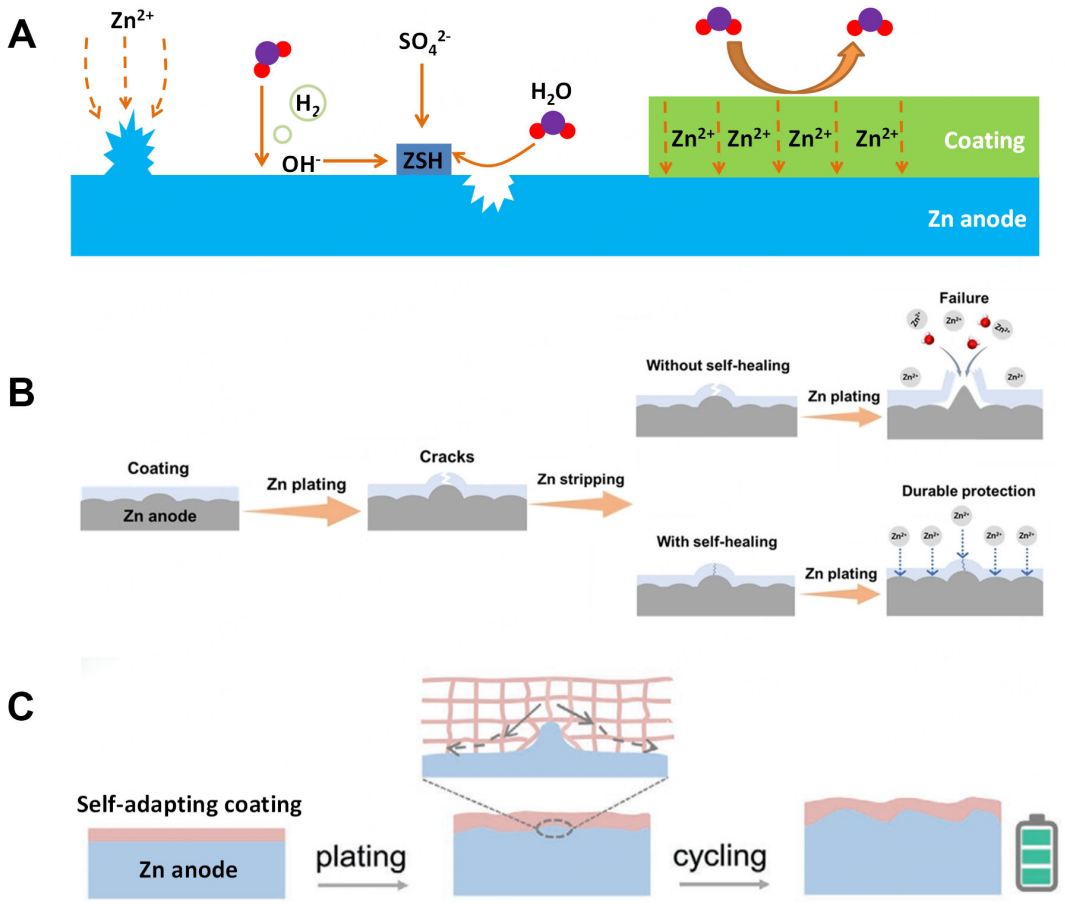

Figure 11. (A) Schematic illustration of action mechanism for the protective coating to achieve stable and planar Zn anode; (B) Schematic illustration of function mechanism for the self-healing coating to achieve durable protection[129]. Copyright 2024 Wiley-VCH GmbH; (C) Schematic illustration of function mechanism for the self-adapting coating[130]. Copyright 2021 Wiley-VCH GmbH.

Under large-capacity cycling, huge volume change and stress can be generated on the interface of Zn anode/protective layer, due to the massive Zn plating/stripping. Therefore, to maintain the long-term function of the artificial protective layer, the self-adapting/self-healing ability is of great importance[129-132], as shown in Figure 11B and C. Through dynamic or reversible chemical interactions, the self-adapting/self-healing coating can be achieved. For instance, Guo *et al.*[130] reported a self-adaptable poly(dimethylsiloxane) (PDMS)/TiO_{2-x} coating to accommodate the volume change and inhibit dendrite growth, in which PDMS possesses high self-adaptability resulting from the dynamic and reversible B-O bonds. Hong *et al.*[131] designed zinc alginate hydrogel as a dynamic coating and Zn^{2+} redistributor on Zn anode via *in-situ* cross-linking effect. Therefore, the Zn anode with a self-adapting interface can accommodate the volume change and repair the possible ruptures to achieve long-term cycling stability. We also constructed a mechanically robust and self-healing protective coating, featured by dual cross-linking dynamic network between SA and Zn^{2+}/lithium polysilicate[132]. On the one hand, the dual cross-linking network with strong mechanical properties is highly resistant to the deformation of Zn anodes. On the other hand, when cracks occur in the network coating, it can effectively self-repair to durably protect the Zn anode.

Electrolyte engineering

Electrolyte design is a promising strategy to suppress the H_2O-induced side reactions and achieve uniform planar Zn deposition. Various electrolyte optimization strategies have been developed, including adjusting

Zn salt type, exploiting functional additives, introducing co-solvents, and constructing eutectic solvents and concentrated electrolytes[133-138]. Exploring electrolyte additives is an economical and scale-up approach to improve the stability of Zn anodes. Figure 12A displays the common functions of the electrolyte additives, including adsorption and shielding, regulating hydrogen bonding network, reconstructing Zn^{2+} solvation structure, and *in-situ* forming SEI film. The electrolyte additives can form a layer of protective film via adsorption or reaction on the Zn surface to shield side reactions and adjust Zn^{2+} flux. Li *et al.*[139] introduced an electrolyte additive N,N-dimethylformamidium trifluoromethanesulfonate (DOTf) in the 2M $ZnSO_4$ aqueous electrolyte. Interestingly, in water, the DOTf is dissociated to neutral ion pairs triflic acid and N,N-dimethylformamide, resulting in the formation of Zn^{2+}-conducting nanostructured SEI on the Zn surface. Such a SEI layer not only excludes H_2O but also induces nanoscale nucleation-growth process of Zn, leading to near 100% coulombic efficiency for the Zn||Cu asymmetric cell under 4 mA cm^{-2}/4 mAh cm^{-2}. Zeng *et al.*[140] reported the *in-situ* formation of a dense and stable SEI layer with high ionic conductivity by introducing $Zn(H_2PO_4)_2$ into the electrolyte. The formed SEI not only hinders the side reactions by isolating Zn anode from the bulk electrolyte but also enables uniform Zn^{2+} transport. Hence, homogeneous Zn deposition and stable Zn plating/stripping have been achieved, as shown in Figure 12B and C. Finally, Figure 12D displays that the Zn||V_2O_5 full cell can give a long cycling lifespan under high loading and low N/P ratio. We also exploited penta-potassium triphosphate (KTPP) as a novel trifunctional electrolyte additive to tune the electrode/electrolyte interface[141]. Firstly, the KTPP electrolyte additive can induce a Zn^{2+}-conducting and mechanically robust protective film on the Zn anode surface. Secondly, the KTPP can complex with Zn^{2+} to reconstitute their dissolution sheath structure. Finally, the K^+ cations from KTPP can adsorb on the Zn anode tips acting as a dynamic shielding layer to regulate Zn^{2+} flux. Consequentially, Zn||Zn symmetric cells achieve dramatically improved cycling stability and a high cumulative capacity of 6,400/7,200 mAh cm^{-2} at 40/20 mA cm^{-2}. Li *et al.*[142] used L-cysteine to construct a self-assembled multilayer, acting as a buffer layer on the Zn surface. The molecular multilayer dynamically replenished the defects caused by the change in electrode morphology during the cycling process, and thus achieved dendrite-free Zn anodes with excellent stability.

The coordinated H_2O within the Zn^{2+} solvation sheath and active free water in the bulk electrolyte cause severe HER and side reactions. Several electrolyte additives/co-solvents have been designed to reconstruct the Zn^{2+} solvation sheath and hydrogen bonding network in the electrolyte[143-148]. For example, You *et al.*[143] presented a cost-effective and eco-friendly aqueous electrolyte consisting of formamide (FA) and zinc acetate. FA, as both a hydrogen bonding acceptor and donor, can powerfully anchor H_2O molecules via a double-site anchoring configuration [Figure 13A] and thereby break the original hydrogen bonding network. As a result, the free water activity is reduced to decrease the HER. Meanwhile, the freezing point of the electrolyte is significantly decreased to < -40 °C [Figure 13B]. Moreover, by adding FA into the electrolyte, uniform Zn deposition can be achieved by regulating the Zn^{2+} solvation structure. As a result, the Zn||Zn symmetric cell and Zn||polyaniline (PANI) full cell with the as-designed electrolyte display impressive cycling stability at -30 °C, as shown in Figure 13C and D. We exploited the sustainable natural disaccharide, D-trehalose (DT), as a multifunctional co-solvent to massively reconstruct Zn^{2+} coordination structure and hydrogen bonding network of the electrolyte[144]. DT molecules contain a great number of polar -OH groups, which can act as a facile platform to form strong interactions with Zn^{2+} and H_2O molecules. Especially, the massive strong hydrogen bonds between DT and H_2O molecules can not only significantly reduce the H_2O activity but also suppress their rearrangement under low temperatures. Consequently, at 5 mA cm^{-2}/5 mAh cm^{-2}, the Zn||Zn symmetric cell using DT30 can stably cycle over 800 h, which is much superior compared to the cell without DT co-solvent.

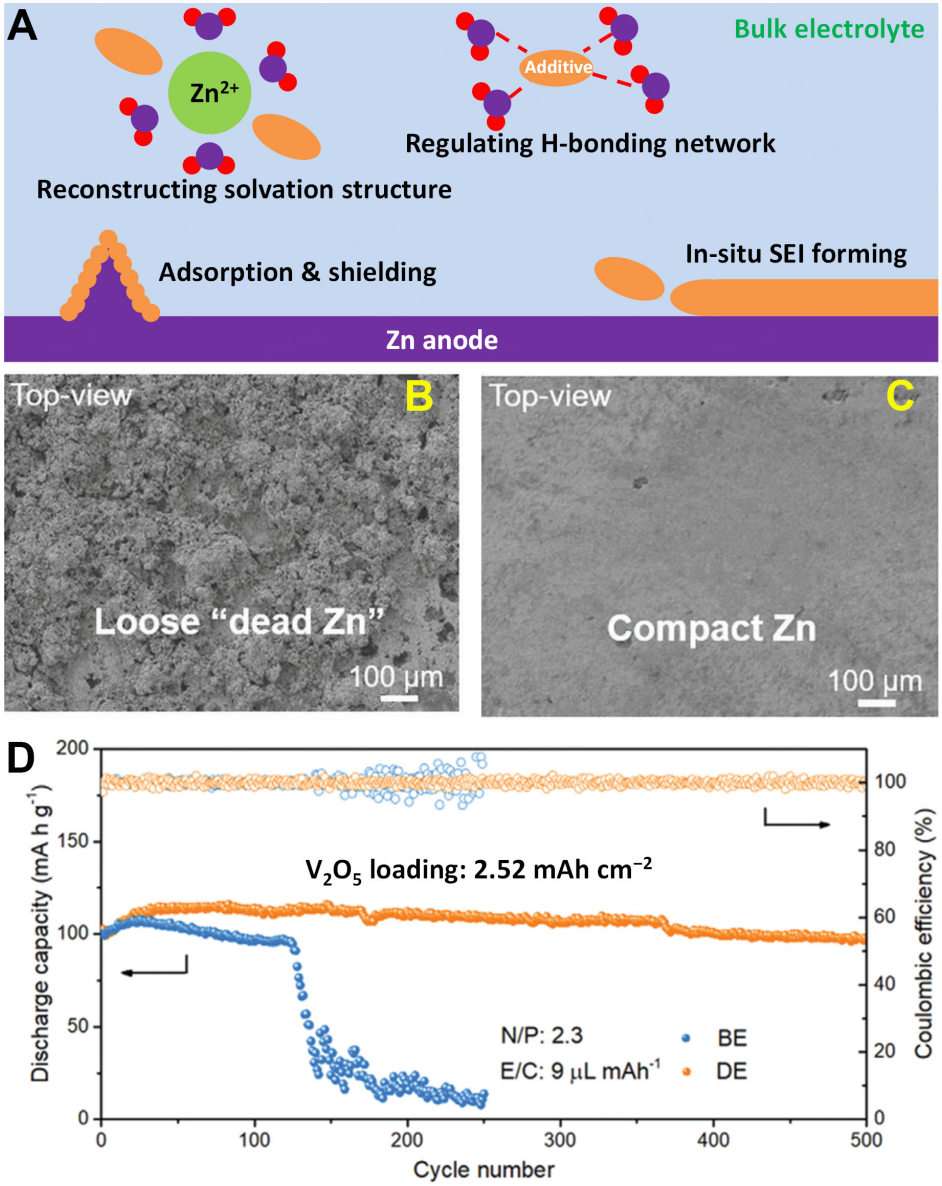

Figure 12. (A) Schematic illustration of function mechanism for the electrolyte additive. SEM images of Zn electrodes after cycling for 400 h in the (B) baseline electrolyte (BE) and (C) the designed electrolyte (DE) at 1 mA cm^{-2}/1 mA h cm^{-2}; (D) Cycling stability of Zn||V_2O_5 cells under practical conditions[140]. Copyright 2021 Wiley-VCH GmbH. SEM: Scanning electron microscopy.

The competitive HER will lead to the localized high-concentration OH^- on the Zn anode surface, which combine with Zn^{2+} and SO_4^{2-} to form ZSH by-products[149-152]. The insoluble ZSH not only covers the active surface of Zn anodes but also causes the loss of active Zn, leading to fast failure of Zn anodes. Moreover, for the practical application of AZIBs, the low N/P ratio is indispensable. The loss of active surface and active Zn is fatal under limited usage of Zn anode in practical AZIBs. To address this issue, we proposed an effective reactivation strategy for the main by-product ZSH on Zn anodes enabled by the catalysis-coordination chemistry[153]. We found that the urea electrolyte additive can preferentially adsorb on the produced ZSH by-products [Figure 14A]. Then, it can suffer from catalytic hydrolysis to generate strong ligand NH_3. The NH_3 rapidly adsorbs on the ZSH surface and coordinates with the Zn^{2+} ion to form soluble $[Zn(NH_3)_4]^{2+}$, resulting in the timely decomposition of ZSH, as shown in Figure 14B. Based on this strategy,

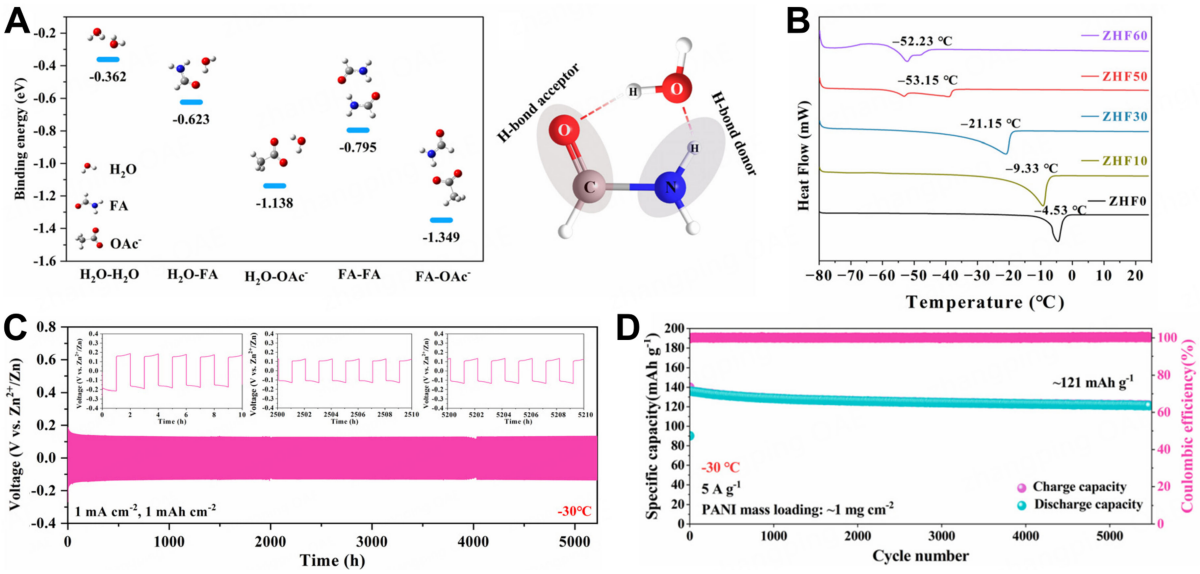

Figure 13. (A) Calculated binding energies of H_2O-H_2O, H_2O-FA, H_2O-OAc^-, FA-FA, and FA-OAc^- pairs; (B) The DSC curves of the electrolytes with different volume ratios of H_2O and FA; Cycling stability with the ZHF50 electrolyte at -30 °C for (C) Zn||Zn cell and (D) Zn||PANI cell[143]. Copyright 2023 The Royal Society of Chemistry. FA: Formamide; DSC: differential scanning calorimetry.

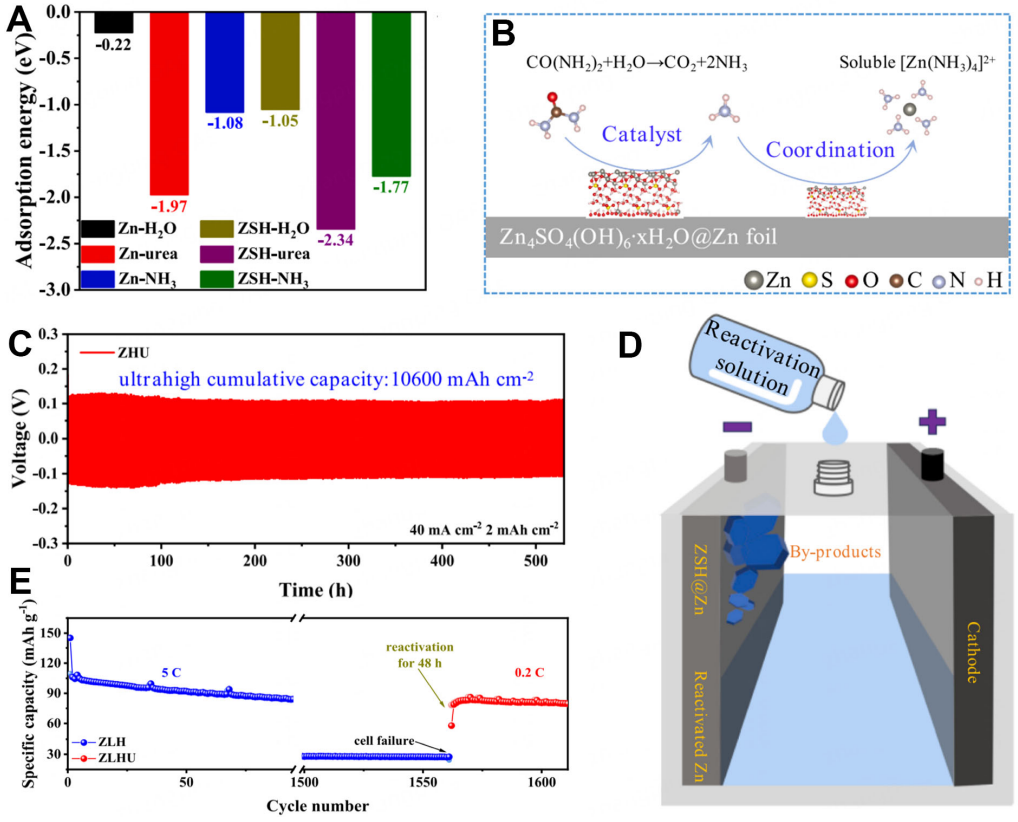

Figure 14. (A) Calculated adsorption energies of H_2O, urea, and NH_3 molecules on the Zn (002) and ZSH (001) crystal planes; (B) Schematic demonstration of the reactivation of ZSH@Zn by urea additive; (C) Cycling stability of Zn||Zn symmetric cell in the designed electrolyte ZHU at 40 mA cm^{-2}/2 mAh cm^{-2}; (D) Model diagram of the reactivation process for the waste battery under practical application; (E) Cycling performance of Zn||$LiFePO_4$ full cell before and after the reactivation[153]. Copyright 2024 Elsevier Inc.

the reversibility of Zn anodes has been obviously improved, and the cumulative capacity of the Zn||Zn symmetric cell reaches as high as 10,600 mAh cm^{-2} at 40 mA cm^{-2} [Figure 14C]. For practical application, the as-prepared electrolyte can act as a reactivation solution to repair the waste AZIBs, as shown in Figure 14D and E.

To match the high-areal-capacity cathodes, this section reviews the recent progress of Zn anodes under large capacity based on surface coating and electrolyte engineering. The artificial surface coating as a solid barrier can effectively shield the active water and regulate the Zn^{2+} flux to achieve uniform and dendrite-free Zn deposition. *In-situ* and ex-situ methods have been developed to construct the functional surface coatings. The Zn^{2+} coordination structure and hydrogen bonding network of the electrolyte can be adjusted by electrolyte engineering to effectively regulate the deposition behavior of Zn and decrease the activity of water. However, under practical conditions, massive Zn stripping/plating can cause huge volume change and internal stress. Therefore, to accommodate the large stress, the mechanical property and self-adapting/self-healing ability of the artificial protective layer should be given considerable attention. For current study, flooded electrolyte is commonly used to achieve optimal cycling stability. Under lean electrolyte, the optimal electrolyte composition should be reevaluated. Under a low N/P ratio, the loss of active Zn will result in fast capacity fading of the AZIBs. Therefore, the development of an effective reactivation strategy for dead Zn is an important and urgent research direction.

CONCLUSION AND OUTLOOK

AZIBs possess the advantages of being low-cost, eco-friendly, and intrinsically safe and have attracted wide attention for their applications in grid electrochemical energy storage systems. To achieve high energy density of AZIBs, constructing high-loading cathodes is the prerequisite, which is a straightforward approach to achieve high areal capacity. However, the high-loading cathodes still face several key issues, including mechanical instability, structural instability, hysteretic charge transfer kinetics, and unmatched Zn anode. To boost the development of high-performance cathodes under high loading, this review summarizes and analyses the main strategies to address the above issues, including (1) rational binder design, (2) 3D cathode design, (3) cathode material structural optimization, and (4) interface engineering for Zn anode. Table 1 displays that prominent improvements have been achieved through rational development strategies. However, to reach the areal-specific capacity of commercial Li-ion batteries (3.0 mAh cm^{-2}), there is still a great gap. High areal-specific capacity and long cycling lifespan can not be achieved at the same time, as shown in Table 1. Therefore, to achieve practical AZIBs, a comprehensive strategy should be devotement rather than single strategy. As shown in Figure 15, the robust multifunctional binder should be elementary to construct high-loading cathodes, and then the electrode microstructure optimization can facilitate fast charge transfer at the electrode level. Material structure and morphology regulation contributes to the improved reaction kinetics to obtain high cathode material availability. Finally, a practical Zn anode is also imperative to maintain the satisfactory cycling performance of the whole AZIBs. We believe this review will provide an in-depth understanding for the rational construction of high-loading cathodes. However, additional efforts should still be made to achieve further progress in the aspects described in the following text.

1. To consider the sustainability and cost-effectiveness, biomass should be one of the promising candidates in large-scale application of AZIBs. For example, bio-polymers have been widely exploited as the polymer binders in Li-ion batteries and Li-S batteries, and should be explored in AZIBs. For future development, the rational molecular design of the bio-polymer binder should be considered to effectively regulate its mechanical/physical properties and integrate multiple functions in one. Moreover, the bio-materials can also be applied in electrode surface coating, electrolyte additive, and hydrogel electrolyte. Finally, the

Table 1. A summary of the electrochemical performance of high-loading cathodes in AZIBs

Strategies and methods	Cathode material/ Mass loading	Electrochemical performance	Ref.
Rational binder design Multifunctional LA133 binder	I_2 7.82 mg cm^{-2}	92.67 mAh g^{-1} (0.72 mAh cm^{-2}) @ 1,000 cycles	[89]
Rational binder design Multifunctional CTS binder	I_2 1-2 mg cm^{-2}	144.1 mAh g^{-1} (~0.29 mAh cm^{-2}) @ 1,500 cycles	[90]
Three-dimensional cathode design Carbon fabric 3D current collector	VO_2 15.0 mg cm^{-2}	228 mAh g^{-1} (3.42 mAh cm^{-2}) @ 50 cycles	[91]
Three-dimensional cathode design CR 3D current collector	CNT/α-MnO_2 10.0 mg cm^{-2}	39.0 mAh g^{-1} (0.39 mAh cm^{-2}) @ 1,000 cycles	[96]
Three-dimensional cathode design 3D-structured active material	VOHAs 5.0 mg cm^{-2}	152 mAh g^{-1} (0.76 mAh cm^{-2}) @ 800 cycles	[97]
Three-dimensional cathode design 3D carbon nanotube network	NMO/VTCNTs 5.0 mg cm^{-2}	329 mAh g^{-1} (1.65 mAh cm^{-2}) @ 120 cycles	[98]
Three-dimensional cathode design 3DP carbon-based current collector	MnO_2 28.4 mg cm^{-2}	282.8 mAh g^{-1} (8.03 mAh cm^{-2}) @ 1st cycle	[103]
Three-dimensional cathode design Direct ink writing technology	FeVO/rHGO 12.4 mg cm^{-2}	126.4 mAh g^{-1} (1.57 mAh cm^{-2}) @ 650 cycles	[104]
Cathode material structural optimization Graphene coating	HAVO@G 15.7 mg cm^{-2}	131.7 mAh g^{-1} (2.07 mAh cm^{-2}) @ 400 cycles	[106]
Cathode material structural optimization MXene surface coating	$Ti_3C_2T_x$@MnO_2 8.0 mg cm^{-2}	287.6 mAh g^{-1} (2.30 mAh cm^{-2}) @ 1st cycle	[110]
Cathode material structural optimization Mn^{2+} ion intercalation	MVOH 19.9 mg cm^{-2}	192.0 mAh g^{-1} (3.82 mAh cm^{-2}) @ 250 cycles	[112]
Cathode material structural optimization Cu doping and Bi-vacancy	Cu-$Bi_{2-x}Se_3$ 10.18 mg cm^{-2}	231.8 mAh g^{-1} (2.36 mAh cm^{-2}) @ 50 cycles	[113]
Cathode material structural optimization Na^+ and Cu^{2+} co-intercalation	NCMO 10.9 mg cm^{-2}	192.7 mAh g^{-1} (2.10 mAh cm^{-2}) @ 50 cycles	[116]
Cathode material structural optimization CTAB molecule intercalation	MoS_2-CTAB 11.5 mg cm^{-2}	75.65 mAh g^{-1} (0.87 mAh cm^{-2}) @ 50 cycles	[118]
Interface engineering for Zn anode Water-glass artificial protective layer	V_2O_5 11.0 mg cm^{-2}	234 mAh g^{-1} (2.57 mAh cm^{-2}) @ 60 cycles	[121]
Interface engineering for Zn anode Self-healing artificial coating	MnO_2 2.91 mg cm^{-2}	175 mAh g^{-1} (0.51 mAh cm^{-2}) @ 400 cycles	[129]
Interface engineering for Zn anode PDMS/TiO_{2-x} self-adaptable coating	MnO_2 1.5 mg cm^{-2}	179 mAh g^{-1} (0.27 mAh cm^{-2}) @ 400 cycles	[130]
Interface engineering for Zn anode $Zn(H_2PO_4)_2$ film-forming additive	V_2O_5 8.7 mg cm^{-2}	98.4 mAh g^{-1} (0.86 mAh cm^{-2}) @ 500 cycles	[140]
Interface engineering for Zn anode $Zn(OAc)_2$/FA-H_2O electrolyte	PANI 3.5 mg cm^{-2}	132 mAh g^{-1} (0.46 mAh cm^{-2}) @ 1st cycle	[143]

AZIBs: Aqueous Zn-ion batteries; CTS: chitosan; CNT: carbon nanotube; VOHAs: $V_3O_7{\cdot}H_2O$ nanoarrays; NMO: $Na_{0.55}Mn_2O_4{\cdot}1.5H_2O$; VTCNTs: varying thinness CNT networks; MVOH: $Mn_{2.5}V_{10}O_{24}{\cdot}5.9H_2O$; NCMO: Na^+ and Cu^{2+} co-intercalated δ-MnO_2; CTAB: $C_{19}H_{42}N^+$; PDMS: poly(dimethylsiloxane); FA: formamide; PANI: polyaniline.

biomass, as a sustainable raw material, can be converted to carbon materials as the conductive host and supporter.

2. Evaluation of the electrochemical performance of the cathodes should shift from the lab to practical conditions. For the cycling stability evaluation of high-loading cathodes, coin cells are usually applied in the past studies, under flood electrolytes and excess Zn anodes. To scale up the lab achievements, the electrochemical performance tests using pouch cells are vital. However, there may be a big gap for the electrochemical performance between coin cells and pouch cells. Therefore, to boost the industrialization of AZIBs, the high-loading cathodes should be evaluated using pouch cells under practical conditions, such as thin Zn anodes and lean electrolytes.

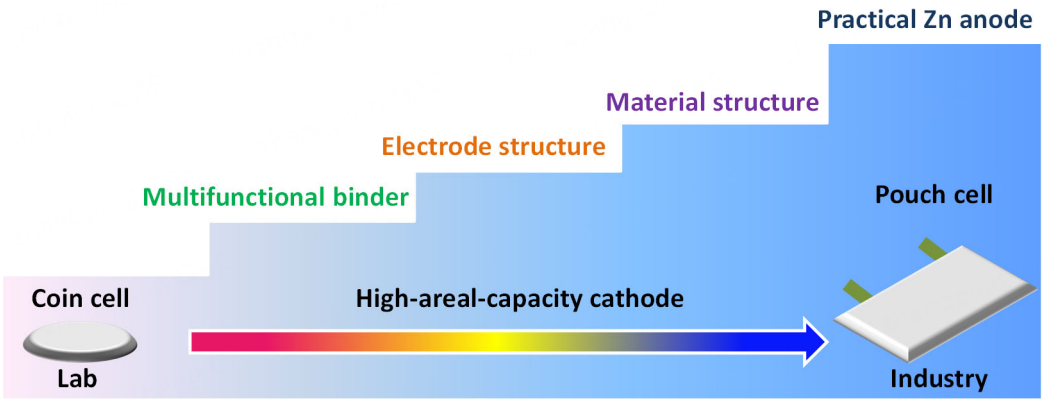

Figure 15. The schematic of a comprehensive solution for constructing practical high-loading cathodes.

3. For the design and pick of functional materials, vast trial-and-error efforts have been made. This results in a long study time and a waste of resources to determine the possible elements and compositions achieving the expected properties. Theoretical calculation has been demonstrated as a powerful tool to study and predict the properties of functional materials. Recently, machine learning, as a hot artificial intelligence technology, has shown significant potential in screening and predicting new materials. Therefore, advanced screening technology should be used to establish standards for functional material prediction and selection.

4. The mechanism study of the functional materials is usually carried out under low-loading conditions. However, the failure mechanism under large-capacity cycling may be different. For example, under large-areal-capacity cycling, the significant volume change/deformation of the electrodes can cause huge stress in electrodes. Therefore, the mechanical coupling mechanism must be considered. Moreover, under a low E/C ratio, can the tiny electrolyte additive work well according to the action mechanism with flooded electrolytes? Therefore, the failure/action mechanism under practical conditions is suggested to be further studied combined with the advanced characterization technology.

5. Finally, a comprehensive performance evaluation of AZIBs should be carried out. In the lab study, the specific capacity and cycling number are widely considered. However, in practical applications, the long-term storage performance of the batteries also needs to be evaluated. In large-scale energy storage applications, intermittent and slow charging processes while fast discharging processes frequently occur. Therefore, slow charging and fast discharging tests of the AZIBs should be performed.

DECLARATIONS

Authors' contributions

Investigation, writing: Wan, J.
Investigation: Song, H.; Tian, J.
Funding acquisition: Zhong, S.
Funding acquisition, conception, writing: Liu, J.

Availability of data and materials

Not applicable.

Financial support and sponsorship

This work was financially supported by the National Natural Science Foundation of China (22005169;

52074099; 52164029) and the Youth Innovation Team Project of Shandong Higher Education Institutions (2022KJ309).

Conflicts of interest

All authors declared that there are no conflicts of interest.

Ethical approval and consent to participate

Not applicable.

Consent for publication

Not applicable.

Copyright

REFERENCES

1. Sharma, R.; Sharda, H.; Dutta, A.; et al. Optimizing green hydrogen production: leveraging load profile simulation and renewable energy integration. *Int. J. Hydrogen. Energy.* **2023**, *48*, 38015-26. DOI
2. Reza, M.; Hannan, M.; Ker, P. J.; et al. Uncertainty parameters of battery energy storage integrated grid and their modeling approaches: a review and future research directions. *J. Energy. Storage.* **2023**, *68*, 107698. DOI
3. Njema, G. G.; Ouma, R. B. O.; Kibet, J. K.; V P. A review on the recent advances in battery development and energy storage technologies. *J. Renew. Energy.* **2024**, *2024*, 2329261. DOI
4. Tian, X.; Yi, Y.; Fang, B.; et al. Design strategies of safe electrolytes for preventing thermal runaway in lithium ion batteries. *Chem. Mater.* **2020**, *32*, 9821-48. DOI
5. Wang, Y.; Wu, Z.; Zhang, R.; et al. Spider silk inspired polymer electrolyte with well bonded interface and fast kinetics for solid-state lithium-ion batteries. *Mater. Today.* **2024**, *76*, 1-8. DOI
6. Wang, M.; Zheng, X.; Zhang, X.; et al. Opportunities of aqueous manganese-based batteries with deposition and stripping chemistry. *Adv. Energy. Mater.* **2021**, *11*, 2002904. DOI
7. Lv, Y.; Geng, X.; Luo, W.; et al. Review on influence factors and prevention control technologies of lithium-ion battery energy storage safety. *J. Energy. Storage.* **2023**, *72*, 108389. DOI
8. Kang, H.; Chen, Q.; Ma, Q.; et al. Coaxial spiral structural polymer/reduced graphene oxide composite as a high-performance anode for potassium ion batteries. *J. Power. Sources.* **2022**, *545*, 231951. DOI
9. Lei, S.; Liu, Z.; Liu, C.; et al. Opportunities for biocompatible and safe zinc-based batteries. *Energy. Environ. Sci.* **2022**, *15*, 4911-27. DOI
10. Fu, M.; Yu, H.; Huang, S.; et al. Building sustainable saturated fatty acid-zinc interfacial layer toward ultra-stable zinc metal anodes. *Nano. Lett.* **2023**, *23*, 3573-81. DOI
11. Wu, Z.; Li, M.; Tian, Y.; et al. Cyclohexanedodecol-assisted interfacial engineering for robust and high-performance zinc metal anode. *Nano-Micro. Lett.* **2022**, *14*, 110. DOI PubMed PMC
12. Zhu, J.; Tie, Z.; Bi, S.; Niu, Z. Towards more sustainable aqueous zinc-ion batteries. *Angew. Chem. Int. Ed.* **2024**, *136*, e202403712. DOI PubMed
13. Gu, X.; Du, Y.; Cao, Z.; et al. Hexamethylenetetramine additive with zincophilic head and hydrophobic tail for realizing ultra-stable Zn anode. *Chem. Eng. J.* **2023**, *460*, 141902. DOI
14. Luo, Z.; Xia, Y.; Chen, S.; et al. Synergistic "anchor-capture" enabled by amino and carboxyl for constructing robust interface of Zn anode. *Nano-Micro. Lett.* **2023**, *15*, 205. DOI PubMed PMC
15. Han, C.; Li, W.; Liu, H. K.; Dou, S.; Wang, J. Principals and strategies for constructing a highly reversible zinc metal anode in aqueous batteries. *Nano. Energy.* **2020**, *74*, 104880. DOI
16. Zhou, M.; Tong, Z.; Li, H.; et al. Regulating preferred crystal plane with modification of exposed grain boundary toward stable Zn anode. *Adv. Funct. Mater.* **2025**, *35*, 2412092. DOI
17. Liu, Z.; Luo, X.; Qin, L.; Fang, G.; Liang, S. Progress and prospect of low-temperature zinc metal batteries. *Adv. Powder. Mate.* **2022**, *1*, 100011. DOI
18. Yi, Z.; Chen, G.; Hou, F.; Wang, L.; Liang, J. Strategies for the stabilization of Zn metal anodes for Zn-ion batteries. *Adv. Energy. Mater.* **2021**, *11*, 2003065. DOI
19. Wang, J.; Yang, Y.; Zhang, Y.; et al. Strategies towards the challenges of zinc metal anode in rechargeable aqueous zinc ion batteries. *Energy. Storage. Mater.* **2021**, *35*, 19-46. DOI
20. Du, W.; Ang, E. H.; Yang, Y.; Zhang, Y.; Ye, M.; Li, C. C. Challenges in the material and structural design of zinc anode towards

high-performance aqueous zinc-ion batteries. *Energy. Environ. Sci.* **2020**, *13*, 3330-60. DOI

21. Zhang, X.; Li, J.; Liu, D.; et al. Ultra-long-life and highly reversible Zn metal anodes enabled by a desolvation and deanionization interface layer. *Energy. Environ. Sci.* **2021**, *14*, 3120-9. DOI
22. Hao, J.; Li, X.; Zhang, S.; et al. Designing dendrite-free Zinc anodes for advanced aqueous zinc batteries. *Adv. Funct. Mater.* **2020**, *30*, 2001263. DOI
23. Liu, Z.; Li, G.; Xi, M.; et al. Interfacial engineering of Zn metal via a localized conjugated layer for highly reversible aqueous zinc ion battery. *Angew. Chem. Int. Ed.* **2024**, *136*, e202319091. DOI
24. Zhou, C.; Shan, L.; Nan, Q.; et al. Construction of robust organic-inorganic interface layer for dendrite-free and durable zinc metal anode. *Adv. Funct. Mater.* **2024**, *34*, 2312696. DOI
25. Li, Y.; Liu, X.; Zhang, M.; et al. Optimization Strategy of surface and interface in electrolyte structure of aqueous zinc-ion battery. *ACS. Mater. Lett.* **2024**, *6*, 1938-60. DOI
26. Huang, S.; Hou, L.; Li, T.; Jiao, Y.; Wu, P. Antifreezing hydrogel electrolyte with ternary hydrogen bonding for high-performance zinc-ion batteries. *Adv. Mater.* **2022**, *34*, 2110140. DOI
27. Wang, R.; Ma, Q.; Zhang, L.; et al. An aqueous electrolyte regulator for highly stable zinc anode under -35 to 65 °C. *Adv. Energy. Mater.* **2023**, *13*, 2302543. DOI
28. Pan, Y.; Liu, Z.; Liu, S.; et al. Quasi-decoupled solid-liquid hybrid electrolyte for highly reversible interfacial reaction in aqueous zinc-manganese battery. *Adv. Energy. Mater.* **2023**, *13*, 2203766. DOI
29. Hu, Y.; Liu, Z.; Li, L.; et al. Reconstructing interfacial manganese deposition for durable aqueous zinc-manganese batteries. *Natl. Sci. Rev.* **2023**, *10*, nwad220. DOI
30. Zong, Q.; Zhuang, Y.; Liu, C.; et al. Dual effects of metal and organic ions Co-intercalation boosting the kinetics and stability of hydrated vanadate cathodes for aqueous zinc-ion batteries. *Adv. Energy. Mater.* **2023**, *13*, 2301480. DOI
31. Li, S.; Shang, J.; Li, M.; et al. Design and synthesis of a π-conjugated N-heteroaromatic material for aqueous zinc-organic batteries with ultrahigh rate and extremely long life. *Adv. Mater.* **2023**, *35*, 2207115. DOI
32. Zeng, Y.; Lu, X. F.; Zhang, S. L.; Luan, D.; Li, S.; Lou, X. W. D. Construction of Co-Mn prussian blue analog hollow spheres for efficient aqueous Zn-ion batteries. *Angew. Chem. Int. Ed.* **2021**, *60*, 22189-94. DOI PubMed PMC
33. Yang, G.; Liang, Z.; Li, Q.; Li, Y.; Tian, F.; Wang, C. Epitaxial core-shell MnFe prussian blue cathode for highly stable aqueous zinc batteries. *ACS. Energy. Lett.* **2023**, *8*, 4085-95. DOI
34. Hu, Y.; Wang, P.; Li, M.; Liu, Z.; Liang, S.; Fang, G. Challenges and industrial considerations towards stable and high-energy-density aqueous zinc-ion batteries. *Energy. Environ. Sci.* **2024**, *17*, 8078-93. DOI
35. Nie, N.; Wang, F.; Yao, W. Fabrication of a 3D structure MnO_2 electrode with high MnO_2 mass loading as the cathode for high-performance aqueous zinc-ion batteries. *Electrochim. Acta.* **2023**, *472*, 143423. DOI
36. Shang, P.; Liu, Y.; Mei, Y.; Wu, L.; Dong, Y. Defective MnO_2 nanosheets based free-standing and high mass loading electrodes for high energy density aqueous zinc ion batteries. *Mater. Chem. Front.* **2021**, *5*, 8002-9. DOI
37. Liu, S.; Zhang, R.; Wang, C.; et al. Zinc ion batteries: bridging the gap from academia to industry for grid-scale energy storage. *Angew. Chem. Int. Ed.* **2024**, *63*, e202400045. DOI
38. Zhou, G.; Chen, H.; Cui, Y. Formulating energy density for designing practical lithium-sulfur batteries. *Nat. Energy.* **2022**, *7*, 312-9. DOI
39. Zeng, Y.; Pei, Z.; Luan, D.; Lou, X. W. D. Atomically dispersed zincophilic sites in N,P-codoped carbon macroporous fibers enable efficient Zn metal anodes. *J. Am. Chem. Soc.* **2023**, *145*, 12333-41. DOI
40. Wen, Y.; Lin, X.; Sun, X.; et al. A biomass-rich, self-healable, and high-adhesive polymer binder for advanced lithium-sulfur batteries. *J. Colloid. Interface. Sci.* **2024**, *660*, 647-56. DOI
41. Liu, H.; Cheng, X.; Chong, Y.; Yuan, H.; Huang, J.; Zhang, Q. Advanced electrode processing of lithium ion batteries: a review of powder technology in battery fabrication. *Particuology* **2021**, *57*, 56-71. DOI
42. Zou, F.; Manthiram, A. A review of the design of advanced binders for high-performance batteries. *Adv. Energy. Mater.* **2020**, *10*, 2002508. DOI
43. Jiang, X.; Wang, T.; Ji, M.; et al. Enhancement of De-solvation kinetics on V_5O_{12}•$6H_2O$ cathode through a Bi-functional modification layer for low-temperature zinc-ion batteries. *Adv. Funct. Mater.* **2025**, *35*, 2420686. DOI
44. Ding, T.; Yu, S.; Feng, Z.; Song, B.; Zhang, H.; Lu, K. Tunable Zn^{2+} de-solvation behavior in MnO_2 cathodes via self-assembled phytic acid monolayers for stable aqueous Zn-ion batteries. *Nanoscale* **2024**, *16*, 21317-25. DOI
45. Liang, W.; Che, Y.; Cai, Z.; et al. Surface decoration manipulating Zn^{2+}/H^+ carrier ratios for hyperstable aqueous zinc ion battery cathode. *Adv. Funct. Mater.* **2024**, *34*, 2304798. DOI
46. Zhu, K.; Wu, T.; Sun, S.; van, B. W.; Stefik, M.; Huang, K. Synergistic H^+/Zn^{2+} dual ion insertion mechanism in high-capacity and ultra-stable hydrated VO_2 cathode for aqueous Zn-ion batteries. *Energy. Storage. Mater.* **2020**, *29*, 60-70. DOI
47. Yu, X.; Yu, D.; Li, Y.; et al. Lattice site substitution and interlayer engineering in layered manganese oxide toward durable and fast aqueous Zn-Mn batteries. *J. Energy. Storage.* **2024**, *93*, 112456. DOI
48. He, L.; Lin, C.; Zeng, L.; et al. Synergistic regulation of anode and cathode interphases via an alum electrolyte additive for high-performance aqueous zinc-vanadium batteries. *Angew. Chem. Int. Ed.* **2025**, *64*, e202415221. DOI
49. Liu, J.; Shen, Z.; Lu, C. Research progress of prussian blue and its analogues for cathodes of aqueous zinc ion batteries. *J. Mater. Chem. A.* **2024**, *12*, 2647-72. DOI

50. Zhang, S.; Fang, M.; Wang, F.; et al. A novel layered ternary metal chalcogenide Bi_2Te_2Se as a high-performance cathode for aqueous zinc ion batteries. *Chem. Eng. J.* **2024**, *496*, 153980. DOI
51. Mahmood, A.; Zheng, Z.; Chen, Y. Zinc-bromine batteries: challenges, prospective solutions, and future. *Adv. Sci.* **2024**, *11*, 2305561. DOI PubMed PMC
52. Huang, L.; Li, J.; Wang, J.; et al. Organic compound as a cathode for aqueous zinc-ion batteries with improved electrochemical performance via multiple active centers. *ACS. Appl. Energy. Mater.* **2022**, *5*, 15780-7. DOI
53. Wu, L.; Li, Z.; Xiang, Y.; et al. Revisiting the charging mechanism of α-MnO_2 in mildly acidic aqueous zinc electrolytes. *Small* **2024**, *20*, 2404583. DOI
54. Ren, Y.; Li, H.; Rao, Y.; Zhou, H.; Guo, S. Aqueous MnO_2/Mn^{2+} electrochemistry in batteries: progress, challenges, and perspectives. *Energy. Environ. Sci.* **2024**, *17*, 425-41. DOI
55. Dai, Y.; Zhang, C.; Li, J.; et al. Inhibition of vanadium cathodes dissolution in aqueous Zn-ion batteries. *Adv. Mater.* **2024**, *36*, 2310645. DOI
56. Yang, P.; Zhang, K.; Liu, S.; et al. Ionic selective separator design enables long-life zinc-iodine batteries via synergistic anode stabilization and polyiodide shuttle suppression. *Adv. Funct. Mater.* **2024**, *34*, 2410712. DOI
57. Zhang, S. J.; Hao, J.; Wu, H.; et al. Toward high-energy-density aqueous zinc-iodine batteries: multielectron pathways. *ACS. Nano.* **2024**, *18*, 28557-74. DOI
58. Li, X.; Li, N.; Huang, Z.; et al. Enhanced redox kinetics and duration of aqueous I_2/I^- conversion chemistry by MXene confinement. *Adv. Mater.* **2021**, *33*, 2006897. DOI
59. Nie, C.; Wang, G.; Wang, D.; et al. Recent progress on zn anodes for advanced aqueous zinc-ion batteries. *Adv. Energy. Mater.* **2023**, *13*, 2300606. DOI
60. Zhou, T.; Huang, R.; Lu, Q.; et al. Recent progress and perspectives on highly utilized Zn metal anode - towards marketable aqueous Zn-ion batteries. *Energy. Storage. Mater.* **2024**, *72*, 103689. DOI
61. Ouyang, K.; Chen, S.; Ling, W.; et al. Synergistic modulation of in-situ hybrid interface construction and pH buffering enabled ultra-stable zinc anode at high current density and areal capacity. *Angew. Chem. Int. Ed.* **2023**, *135*, e202311988. DOI
62. Li, M.; Wang, X.; Meng, J.; et al. Comprehensive understandings of hydrogen bond chemistry in aqueous batteries. *Adv. Mater.* **2024**, *36*, 2308628. DOI
63. He, Q.; Ning, J.; Chen, H.; et al. Achievements, challenges, and perspectives in the design of polymer binders for advanced lithium-ion batteries. *Chem. Soc. Rev.* **2024**, *53*, 7091-157. DOI
64. Sudhakaran, S.; Bijoy, T. K. A comprehensive review of current and emerging binder technologies for energy storage applications. *ACS. Appl. Energy. Mater.* **2023**, *6*, 11773-94. DOI
65. Liu, J.; Galpaya, D. G. D.; Yan, L.; et al. Exploiting a robust biopolymer network binder for an ultrahigh-areal-capacity Li-S battery. *Energy. Environ. Sci.* **2017**, *10*, 750-5. DOI
66. Qi, Q.; Lv, X.; Lv, W.; Yang, Q. Multifunctional binder designs for lithium-sulfur batteries. *J. Energy. Chem.* **2019**, *39*, 88-100. DOI
67. Yu, D.; Zhang, Q.; Liu, J.; Guo, Z.; Wang, L. A mechanically robust and high-wettability multifunctional network binder for high-loading Li-S batteries with an enhanced rate property. *J. Mater. Chem. A.* **2021**, *9*, 22684-90. DOI
68. Guo, R.; Yang, Y.; Huang, X. L.; et al. Recent advances in multifunctional binders for high sulfur loading lithium-sulfur batteries. *Adv. Funct. Mater.* **2024**, *34*, 2307108. DOI
69. Ling, M.; Xu, Y.; Zhao, H.; et al. Dual-functional gum arabic binder for silicon anodes in lithium ion batteries. *Nano. Energy.* **2015**, *12*, 178-85. DOI
70. Sun, R.; Hu, J.; Shi, X.; et al. Water-soluble cross-linking functional binder for low-cost and high-performance lithium-sulfur batteries. *Adv. Funct. Mater.* **2021**, *31*, 2104858. DOI
71. Xie, D.; Zhao, J.; Jiang, Q.; et al. A high-performance alginate hydrogel binder for aqueous zn-ion batteries. *Chemphyschem* **2022**, *23*, e202200106. DOI
72. Niu, B.; Wang, J.; Guo, Y.; et al. Polymers for aqueous zinc-ion batteries: from fundamental to applications across core components. *Adv. Energy. Mater.* **2024**, *14*, 2303967. DOI
73. Patra, N.; Ramesh, P.; Donthu, V.; Ahmad, A. Biopolymer-based composites for sustainable energy storage: recent developments and future outlook. *J. Mater. Sci. Mater. Eng.* **2024**, *19*, 34. DOI
74. Salleh, N. A.; Kheawhom, S.; Ashrina, A. H. N.; Rahiman, W.; Mohamad, A. A. Electrode polymer binders for supercapacitor applications: a review. *J. Mater. Res. Technol.* **2023**, *23*, 3470-91. DOI
75. Gao, Q.; Shen, Z.; Guo, Z.; et al. Metal coordinated polymer as three-dimensional network binder for high sulfur loading cathode of lithium-sulfur battery. *Small* **2023**, *19*, 2301344. DOI
76. Wang, D.; Zhang, Q.; Liu, J.; et al. A universal cross-linking binding polymer composite for ultrahigh-loading Li-ion battery electrodes. *J. Mater. Chem. A.* **2020**, *8*, 9693-700. DOI
77. Zhao, E.; Guo, Z.; Liu, J.; et al. A low-cost and eco-friendly network binder coupling stiffness and softness for high-performance Li-ion batteries. *Electrochim. Acta.* **2021**, *387*, 138491. DOI
78. Gao, R.; Zhang, Q.; Zhao, Y.; et al. Regulating polysulfide redox kinetics on a self-healing electrode for high-performance flexible lithium-sulfur batteries. *Adv. Funct. Mater.* **2022**, *32*, 2110313. DOI
79. Kovalenko, I.; Zdyrko, B.; Magasinski, A.; et al. A major constituent of brown algae for use in high-capacity Li-ion batteries. *Science* **2011**, *334*, 75-9. DOI

80. Zhang, J.; Wang, N.; Zhang, W.; et al. A cycling robust network binder for high performance Si-based negative electrodes for lithium-ion batteries. *J. Colloid. Interface. Sci.* **2020**, *578*, 452-60. DOI
81. Xu, Y.; Zhang, M.; Tang, R.; et al. A plant root cell-inspired interphase layer for practical aqueous zinc-iodine batteries with super-high areal capacity and long lifespan. *Energy. Environ. Sci.* **2024**, *17*, 6656-65. DOI
82. Dong, H.; Liu, R.; Hu, X.; et al. Cathode-electrolyte interface modification by binder engineering for high-performance aqueous zinc-ion batteries. *Adv. Sci.* **2023**, *10*, 2205084. DOI
83. Peng, Z.; Feng, Z.; Zhou, X.; et al. Polymer engineering for electrodes of aqueous zinc ion batteries. *J. Energy. Chem.* **2024**, *91*, 345-69. DOI
84. Tolstopyatova, E. G.; Kamenskii, M. A.; Kondratiev, V. V. Vanadium oxide-conducting polymers composite cathodes for aqueous zinc-ion batteries: interfacial design and enhancement of electrochemical performance. *Energies* **2022**, *15*, 8966. DOI
85. Kamenskii, M. A.; Volkov, F. S.; Eliseeva, S. N.; Holze, R.; Kondratiev, V. V. Comparative study of PEDOT- and PEDOT:PSS modified δ-MnO_2 cathodes for aqueous zinc batteries with enhanced properties. *J. Electrochem. Soc.* **2023**, *170*, 010505. DOI
86. Yan, L.; Zhang, S.; Kang, Q.; et al. Iodine conversion chemistry in aqueous batteries: challenges, strategies, and perspectives. *Energy. Storage. Mater.* **2023**, *54*, 339-65. DOI
87. Chen, H.; Li, X.; Fang, K.; Wang, H.; Ning, J.; Hu, Y. Aqueous zinc-iodine batteries: from electrochemistry to energy storage mechanism. *Adv. Energy. Mater.* **2023**, *13*, 2302187. DOI
88. Ma, J.; Wang, M.; Zhang, H.; et al. Accelerating the electrochemical kinetics of metal-iodine batteries: progress and prospects. *Mater. Today. Energy.* **2022**, *30*, 101146. DOI
89. Wang, K.; Li, H.; Xu, Z.; et al. An Iodine-chemisorption binder for high-loading and shuttle-free Zn-iodine batteries. *Adv. Energy. Mater.* **2024**, *14*, 2304110. DOI
90. Yang, J. L.; Liu, H. H.; Zhao, X. X.; et al. Janus binder chemistry for synchronous enhancement of iodine species adsorption and redox kinetics toward sustainable aqueous Zn-I_2 batteries. *J. Am. Chem. Soc.* **2024**, *146*, 6628-37. DOI
91. Ma, L.; Wang, X.; Sun, J. A strategy associated with conductive binder and 3D current collector for aqueous zinc-ion batteries with high mass loading. *J. Electroanal. Chem.* **2020**, *873*, 114395. DOI
92. Xue, M.; Bai, J.; Wu, M.; He, Q.; Zhang, Q.; Chen, L. Carbon-assisted anodes and cathodes for zinc ion batteries: from basic science to specific applications, opportunities and challenges. *Energy. Storage. Mater.* **2023**, *62*, 102940. DOI
93. Zheng, W.; Zhu, L.; Huang, H.; Sun, Z.; Zhou, H.; Zhang, K. Achieving high performance aqueous Zn-ion batteries via interfacial coating of N, P dual-doped biomass porous carbon on Zn metal anode. *ACS. Sustain. Chem. Eng.* **2024**, *12*, 8070-82. DOI
94. Liu, X.; Shen, X.; Chen, T.; Xu, Q. The spinel $MnFe_2O_4$ grown in biomass-derived porous carbons materials for high-performance cathode materials of aqueous zinc-ion batteries. *J. Alloys. Compd.* **2022**, *904*, 164002. DOI
95. Wei, L.; Li, X.; Peng, J.; Chen, C.; Li, Z.; Zhao, G. Green synthesis of renewable biomass-derived porous carbon hosts for superior aqueous zinc-iodine batteries. *Inorg. Chem. Commun.* **2024**, *170*, 113489. DOI
96. Zhao, H.; Chen, M.; Yu, J.; et al. Three-dimensional rattan-derived electrodes with directional channels and large mass loadings for high-performance aqueous zinc-ion batteries. *J. Colloid. Interface. Sci.* **2025**, *678*, 441-8. DOI
97. Chen, D.; Lu, M.; Wang, B.; et al. High-mass loading $V_3O_7{\cdot}H_2O$ nanoarray for Zn-ion battery: new synthesis and two-stage ion intercalation chemistry. *Nano. Energy.* **2021**, *83*, 105835. DOI
98. Gao, X.; Zhang, C.; Dai, Y.; et al. Three-dimensional manganese oxide@carbon networks as free-standing, high-loading cathodes for high-performance Zinc-ion batteries. *Small. Struct.* **2023**, *4*, 2200316. DOI
99. Pan, R.; Zheng, A.; He, B.; et al. *In situ* crafting of a 3D N-doped carbon/defect-rich $V_2O_{5-x}{\cdot}nH_2O$ nanosheet composite for high performance fibrous flexible Zn-ion batteries. *Nanoscale. Horiz.* **2022**, *7*, 1501-12. Available from: https://pubs.rsc.org/en/content/articlelanding/2022/nh/d2nh00349j [Last accessed on 18 Apr 2025]
100. Li, Y.; Zhang, F.; Wu, M.; et al. *In situ* growth of δ-MnO_2/C fibers as a binder-free and free-standing cathode for advanced aqueous Zn-ion batteries. *Inorg. Chem. Front.* **2024**, *11*, 8016-24. DOI
101. Peng, J.; Gou, W.; Jiang, T.; et al. 3D printed reticular manganese dioxide cathode with high areal capacity for aqueous zinc ion batteries. *J. Alloys. Compd.* **2024**, *998*, 174772. DOI
102. Ji, D.; Zheng, H.; Zhang, H.; Liu, W.; Ding, J. Coaxial 3D-printing constructing all-in-one fibrous lithium-, sodium-, and zinc-ion batteries. *Chem. Eng. J.* **2022**, *433*, 133815. DOI
103. Yang, H.; Wan, Y.; Sun, K.; et al. Reconciling mass loading and gravimetric performance of MnO_2 cathodes by 3D-printed carbon structures for zinc-ion batteries. *Adv. Funct. Mater.* **2023**, *33*, 2215076. DOI
104. Ma, H.; Tian, X.; Wang, T.; et al. Tailoring pore structures of 3D printed cellular high-loading cathodes for advanced rechargeable zinc-ion batteries. *Small* **2021**, *17*, 2100746. DOI
105. He, Y.; Pu, Y.; Zheng, Y.; et al. Carbon nanofiber-coated MnO composite as high-performance cathode material for aqueous zinc-ion batteries. *J. Phys. Chem. Solids.* **2024**, *184*, 111669. DOI
106. Zhang, W.; Liang, S.; Fang, G.; Yang, Y.; Zhou, J. Ultra-high mass-loading cathode for aqueous zinc-ion battery based on graphene-wrapped aluminum vanadate nanobelts. *Nano-Micro. Lett.* **2019**, *11*, 69. DOI PubMed PMC
107. Xu, H.; Du, Y.; Emin, A.; et al. Interconnected vertical δ-MnO_2 nanoflakes coated by a dopamine-derived carbon thin shell as a high-performance self-supporting cathode for aqueous zinc ion batteries. *J. Electrochem. Soc.* **2021**, *168*, 030540. DOI
108. Luo, Z.; Zeng, J.; Liu, Z.; He, H. Carbon-coated hydrated vanadium dioxide for high-performance aqueous zinc-ion batteries. *J. Alloys. Compd.* **2022**, *906*, 164388. DOI

109. Venkatkarthick, R.; Rodthongkum, N.; Zhang, X.; et al. Vanadium-based oxide on two-dimensional vanadium carbide MXene (V_2O_x@V_2CT_x) as cathode for rechargeable aqueous zinc-ion batteries. *ACS. Appl. Energy. Mater.* **2020**, *3*, 4677-89. DOI
110. Shi, M.; Wang, B.; Chen, C.; Lang, J.; Yan, C.; Yan, X. 3D high-density MXene@MnO_2 microflowers for advanced aqueous zinc-ion batteries. *J. Mater. Chem. A.* **2020**, *8*, 24635-44. DOI
111. Yang, J.; Li, J.; Li, Y.; et al. Defect regulation in bimetallic oxide cathodes for significantly improving the performance of flexible aqueous Zn-ion batteries. *Chem. Eng. J.* **2023**, *468*, 143600. DOI
112. Yang, L.; Zhu, Y.; Zeng, F.; et al. Synchronously promoting the electron and ion transport in high-loading $Mn_{2.5}V_{10}O_{24}$·5.9H_2O cathodes for practical aqueous zinc-ion batteries. *Energy. Storage. Mater.* **2024**, *65*, 103162. DOI
113. Zong, Y.; Chen, H.; Wang, J.; et al. Cation defect-engineered boost fast kinetics of two-dimensional topological Bi_2Se_3 cathode for high-performance aqueous Zn-ion batteries. *Adv. Mater.* **2023**, *35*, 2306269. DOI
114. Zeng, X.; Gong, Z.; Wang, C.; Cullen, P. J.; Pei, Z. Vanadium-based cathodes modification via defect engineering: strategies to support the leap from lab to commercialization of aqueous zinc-ion batteries. *Adv. Energy. Mater.* **2024**, *14*, 2401704. DOI
115. Cui, X.; Li, Y.; Zhang, Y.; et al. Unraveling the electrochemical charge storage dynamics of defective oxides-based cathodes toward high-performance aqueous zinc-ion batteries. *Chem. Eng. J.* **2023**, *478*, 147197. DOI
116. Gao, X.; Shen, C.; Dong, H.; et al. Co-intercalation strategy for simultaneously boosting two-electron conversion and bulk stabilization of Mn-based cathodes in aqueous zinc-ion batteries. *Energy. Environ. Sci.* **2024**, *17*, 2287-97. DOI
117. He, W.; Meng, C.; Ai, Z.; et al. Achieving fast ion diffusion in aqueous zinc-ion batteries by cathode reconstruction design. *Chem. Eng. J.* **2023**, *454*, 140260. DOI
118. Yao, Z.; Zhang, W.; Ren, X.; et al. A volume self-regulation MoS_2 superstructure cathode for stable and high mass-loaded Zn-ion storage. *ACS. Nano.* **2022**, *16*, 12095-106. DOI
119. Zhao, X.; Mao, L.; Cheng, Q.; et al. Interlayer engineering of preintercalated layered oxides as cathode for emerging multivalent metal-ion batteries: zinc and beyond. *Energy. Storage. Mater.* **2021**, *38*, 397-437. DOI
120. Jiang, N.; Zeng, Y.; Yang, Q.; et al. Deep ion mass transfer addressing the capacity shrink challenge of aqueous Zn|MnO_2 batteries during the cathode scaleup. *Energy. Environ. Sci.* **2024**, *17*, 8904-14. DOI
121. Zhu, Y.; Huang, Z.; Zheng, M.; et al. Scalable construction of multifunctional protection layer with low-cost water glass for robust and high-performance zinc anode. *Adv. Funct. Mater.* **2024**, *34*, 2306085. DOI
122. Hong, L.; Wu, X.; Wang, L. Y.; et al. Highly reversible zinc anode enabled by a cation-exchange coating with Zn-ion selective channels. *ACS. Nano.* **2022**, *16*, 6906-15. DOI
123. Li, W.; Zhang, Q.; Yang, Z.; et al. Isotropic amorphous protective layer with uniform interfacial zincophobicity for stable zinc anode. *Small* **2022**, *18*, 2205667. DOI
124. Wang, Z.; Zhou, D.; Zhou, Z.; et al. Synergistic effect of 3D elastomer/super-ionic conductor hybrid fiber networks enables zinc anode protection for aqueous zinc-ion batteries. *Adv. Funct. Mater.* **2024**, *34*, 2313371. DOI
125. Chen, A.; Zhao, C.; Gao, J.; et al. Multifunctional SEI-like structure coating stabilizing Zn anodes at a large current and capacity. *Energy. Environ. Sci.* **2023**, *16*, 275-84. DOI
126. Zhang, Q.; Su, Y.; Shi, Z.; Yang, X.; Sun, J. Artificial interphase layer for stabilized Zn anodes: progress and prospects. *Small* **2022**, *18*, 2203583. DOI
127. Li, J.; Yin, X.; Duan, F.; et al. Pure amorphous and ultrathin phosphate layer with superior ionic conduction for zinc anode protection. *ACS. Nano.* **2023**, *17*, 20062-72. DOI
128. Zhou, X.; Chen, R.; Cui, E.; et al. A novel hydrophobic-zincophilic bifunctional layer for stable Zn metal anodes. *Energy. Storage. Mater.* **2023**, *55*, 538-45. DOI
129. Qiao, L.; Zhang, P.; Yu, Y.; et al. Constructing dynamic cross-linking networks as durable bifunctional coating for highly stable zinc anodes. *Chem. Eur. J.* **2024**, *30*, e202401693. DOI
130. Guo, Z.; Fan, L.; Zhao, C.; et al. A dynamic and self-adapting interface coating for stable Zn-metal anodes. *Adv. Mater.* **2022**, *34*, 2105133. DOI
131. Hong, L.; Wu, X.; Liu, Y.; et al. Self-adapting and self-healing hydrogel interface with fast Zn^{2+} transport kinetics for highly reversible Zn anodes. *Adv. Funct. Mater.* **2023**, *33*, 2300952. DOI
132. Zhang, P.; Yu, Y.; Zhai, R.; et al. Achieving planar Zn deposition enabled by an eco-friendly and mechanically robust dual cross-linking dynamic network coating for long-lifespan Zn-ion batteries. *ACS. Appl. Energy. Mater.* **2024**, *7*, 4160-9. DOI
133. Du, H.; Dong, Y.; Li, Q. J.; et al. A new zinc salt chemistry for aqueous zinc-metal batteries. *Adv. Mater.* **2023**, *35*, 2210055. DOI
134. Zhang, J.; Liu, Y.; Wang, Y.; Zhu, Z.; Yang, Z. Zwitterionic organic multifunctional additive stabilizes electrodes for reversible aqueous Zn-ion batteries. *Adv. Funct. Mater.* **2024**, *34*, 2401889. DOI
135. Liu, Z.; Wang, R.; Ma, Q.; et al. A dual-functional organic electrolyte additive with regulating suitable overpotential for building highly reversible aqueous zinc ion batteries. *Adv. Funct. Mater.* **2024**, *34*, 2214538. DOI
136. Li, Z.; Liao, Y.; Wang, Y.; et al. A co-solvent in aqueous electrolyte towards ultralong-life rechargeable zinc-ion batteries. *Energy. Storage. Mater.* **2023**, *56*, 174-82. DOI
137. Chen, Z.; Zhou, W.; Zhao, S.; Lou, X.; Chen, S. In-situ construction of solid electrolyte interphases with gradient zincophilicity for wide temperature zinc ion batteries. *Adv. Energy. Mater.* **2025**, *15*, 2404108. DOI
138. Dai, Q.; Li, L.; Tu, T.; Zhang, M.; Song, L. An appropriate Zn^{2+}/Mn^{2+} concentration of the electrolyte enables superior performance of AZIBs. *J. Mater. Chem. A.* **2022**, *10*, 23722-30. DOI

139. Li, C.; Shyamsunder, A.; Hoane, A. G.; et al. Highly reversible Zn anode with a practical areal capacity enabled by a sustainable electrolyte and superacid interfacial chemistry. *Joule* **2022**, *6*, 1103-20. DOI
140. Zeng, X.; Mao, J.; Hao, J.; et al. Electrolyte design for in situ construction of highly Zn^{2+} -conductive solid electrolyte interphase to enable high-performance aqueous Zn-ion batteries under practical conditions. *Adv. Mater.* **2021**, *33*, 2007416. DOI
141. Yu, Y.; Zhang, P.; Wang, W.; Liu, J. Tuning the electrode/electrolyte interface enabled by a trifunctional inorganic oligomer electrolyte additive for highly stable and high-rate Zn anodes. *Small. Methods.* **2023**, *7*, 2300546. DOI
142. Li, D.; Tang, Y.; Liang, S.; Lu, B.; Chen, G.; Zhou, J. Self-assembled multilayers direct a buffer interphase for long-life aqueous zinc-ion batteries. *Energy. Environ. Sci.* **2023**, *16*, 3381-90. DOI
143. You, C.; Wu, R.; Yuan, X.; et al. An inexpensive electrolyte with double-site hydrogen bonding and a regulated Zn^{2+} solvation structure for aqueous Zn-ion batteries capable of high-rate and ultra-long low-temperature operation. *Energy. Environ. Sci.* **2023**, *16*, 5096-107. DOI
144. Yu, Y.; Zhang, Q.; Zhang, P.; et al. Massively reconstructing hydrogen bonding network and coordination structure enabled by a natural multifunctional Co-solvent for practical aqueous Zn-ion batteries. *Adv. Sci.* **2024**, *11*, 2400336. DOI
145. Jia, H.; Jiang, X.; Wang, Y.; Lam, Y.; Shi, S.; Liu, G. Hybrid Co-solvent-induced high-entropy electrolyte: regulating of hydrated Zn^{2+} solvation structures for excellent reversibility and wide temperature adaptability. *Adv. Energy. Mater.* **2024**, *14*, 2304285. DOI
146. Wang, H.; Wang, K.; Jing, E.; et al. Strategies of regulating Zn^{2+} solvation structures toward advanced aqueous zinc-based batteries. *Energy. Storage. Mater.* **2024**, *70*, 103451. DOI
147. Li, L.; Jiang, G.; Li, M.; et al. Ether-water Co-solvent electrolytes enhanced vanadium oxide cathode cyclic behaviors for zinc batteries. *ChemSusChem* **2024**, *17*, e202301833. DOI
148. Qiu, K.; Ma, G.; Wang, Y.; et al. Highly compact zinc metal anode and wide-temperature aqueous electrolyte enabled by acetamide additives for deep cycling Zn batteries. *Adv. Funct. Mater.* **2024**, *34*, 2313358. DOI
149. Zhou, S.; Meng, X.; Chen, Y.; et al. Zinc-ion anchor induced highly reversible Zn anodes for high performance Zn-ion batteries. *Angew. Chem. Int. Ed.* **2024**, *136*, e202403050. DOI
150. Huang, Y.; Zhuang, Y.; Guo, L.; et al. Stabilizing anode-electrolyte interface for dendrite-free Zn-ion batteries through orientational plating with zinc aspartate additive. *Small* **2024**, *20*, 2306211. DOI
151. Zhang, Z.; Zhang, Y.; Ye, M.; et al. Lithium bis(oxalate)borate additive for self-repairing zincophilic solid electrolyte interphases towards ultrahigh-rate and ultra-stable zinc anodes. *Angew. Chem. Int. Ed.* **2023**, *62*, e202311032. DOI
152. Cao, H.; Zhang, X.; Xie, B.; et al. Unraveling the solvation structure and electrolyte interface through carbonyl chemistry for durable and dendrite-free Zn anode. *Adv. Funct. Mater.* **2023**, *33*, 2305683. DOI
153. Yu, Y.; Jia, X.; Zhang, Q.; et al. Achieving high-durability aqueous Zn-ion batteries enabled by reanimating inactive Zn on Zn anodes. *J. Colloid. Interface. Sci.* **2025**, *677*, 748-55. DOI